Marine Geology 444 (2022) 106709

Contents lists available at ScienceDirect

Marine Geology

journal homepage: www.elsevier.com/locate/margo

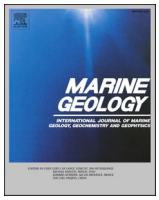

Research Article

Gravel barrier resilience to future sea level rise and storms

J.A. Pollard [a,*], E.K. Christie [a], T. Spencer [a], S.M. Brooks [b]

[a] Cambridge Coastal Research Unit, Department of Geography, University of Cambridge, Downing Place, Cambridge CB2 3EN, UK
[b] Department of Geography, Birkbeck, University of London, Malet Street, London WC1E 7HX, UK

ARTICLE INFO

Editor: Edward Anthony

Keywords:
Coastal resilience
Gravel barrier
Storm surge
Sea level rise
Coastal risk

ABSTRACT

Globally, communities, ecosystems, and assets situated within the coastal zone will likely experience increased risk in the future owing to chronic and acute pressures associated with climate change and accompanying sea level rise. Gravel barrier islands represent an intermediate pathway between seaward hazards and vulnerable landward receptors and possess inherent morpho-sedimentary characteristics which allow coastal risk reduction functions. If gravel barriers are to be usefully and reliably integrated into broader coastal risk management strategies, there is a need to understand the extent to which these landforms are likely to remain resilient under future environmental conditions. Using the Blakeney Point Barrier System, southern North Sea, this study investigates the resilience of gravel barrier landforms to storm surge conditions under future sea level rise scenarios. Resilience is assessed through reference to barrier resistance, susceptibility to state change, persistence, and continued functional performance. Numerical modelling reveals that variable pre-surge barrier morphologies result in a spectrum of episodic resilience trajectories along the barrier frontage. This study also considers the role of humans in altering landscape resilience, demonstrating that previously managed barrier sections (through reprofiling to steepen and heighten the barrier) are more vulnerable to severe morphological change, and associated landward overtopping volume, compared to unmanaged barrier sections. This said, under moderate to high sea level rise, even unmanaged barrier sections failed to demonstrate resilience to storm surge forcing. Such insights help temper our expectations regarding the coastal erosion and flood risk reduction functions of gravel barriers in the face of global environmental change.

1. Introduction

Globally, communities, ecosystems, and assets situated within the coastal zone will likely experience increased risk in the future owing to chronic and acute pressures associated with climate change and accompanying sea level rise (Hinkel et al., 2018). Projections of coastal population growth and land-use change suggest that by 2060 the low elevation coastal zone (defined as 'the contiguous area along the coast that is less than 10 metres above sea level' (McGranahan et al., 2007)) population will more than double, reaching 1.4 billion (Neumann et al., 2015). The coastal hazards to which these populations will be exposed are also intensifying. Hazards include coastal flooding (Vitousek et al., 2017), erosion (Ranasinghe et al., 2012), saltwater intrusion (Ranjan et al., 2009) and ecosystem deterioration (Schuerch et al., 2018). To better mitigate and adapt to the consequences of global environmental change at the coast, a comprehensive understanding of the pathways which connect seaward hazards with vulnerable landward receptors is critically important (Narayan et al., 2012; Sayers et al., 2002).

Barrier islands represent one such pathway. Un-attached and mainland-attached barrier islands occur on 15% of open ocean coasts (Cooper et al., 2018). Gravel barriers are particularly associated with paraglacial coasts (Forbes and Syvitski, 1994); in the Arctic Ocean alone, barriers on such coasts account for 10% of total barrier length globally (Stutz and Pilkey, 2011). Gravel barriers possess inherent morpho-sedimentary characteristics (e.g. coarse-grained composition and steep seaward slopes) which confer coastal risk reduction functions (Masselink and Van Heteren, 2014). To maintain and enhance risk reduction functions, humans have often actively intervened to modify gravel barrier morphology. Such actions include reprofiling to maintain barrier crest elevation and position (Orford et al., 2003), barrier beach nourishment (Bergillos et al., 2017; Hudson and Baily, 2018), and the construction of hard defences on and around such features (Stéphan et al., 2012). However, if gravel barriers are to fulfil their potential as 'highly efficient and practical forms of coastal protection and flood defence'

* Corresponding author.
E-mail addresses: jpollard250@gmail.com (J.A. Pollard), elizabeth.k.christie@gmail.com (E.K. Christie), ts111@cam.ac.uk (T. Spencer), s.brooks@bbk.ac.uk (S.M. Brooks).

https://doi.org/10.1016/j.margeo.2021.106709
Received 13 July 2021; Received in revised form 10 December 2021; Accepted 14 December 2021
Available online 21 December 2021

(EurOtop, 2018, 190), it is important that those responsible for integrating these landforms into coastal risk management strategies understand the extent to which gravel barrier landforms are likely to remain resilient under future environmental conditions (Naylor et al., 2017).

'Resilience' is a term that can be broadly defined and is consequently characterised by diverse usage (Thoms et al., 2018). It is possible to distinguish between 'engineering' and 'ecological' definitions of resilience (Holling, 1996). Engineering resilience assumes a single system state and may be measured by i) how far a system is disturbed from its initial state and ii) how quickly the system can recover to re-assume its initial state. Ecological resilience incorporates multiple plausible system states, separated by non-linear thresholds. It may be measured by i) how much disturbance is required for a threshold to be exceeded and ii) the extent to which system function is maintained under alternative system states. Observations of coastal dynamics suggest that the 'ecological resilience' definition is better suited to describing and quantifying resilience in coastal systems, compared to the engineering paradigm (Kombiadou et al., 2019; Masselink and Lazarus, 2019; Orford and Anthony, 2011; Piégay et al., 2018).

This study defines gravel barrier resilience as comprising a number of elements (Table 1). This definition of resilience is sufficiently flexible as to consider system response to acute, extreme disturbances ('resistance' and 'susceptibility to state change') and longer-term, chronic pressures ('persistence'), whilst acknowledging the socio-ecological nature of many such barrier environments and the consequent importance of system function ('function'). To some extent, the elements of resilience listed in Table 1 are interdependent. For example, systems characterised by higher resistance will typically be less susceptible to state change, which in turn enhances longer term persistence, thus ensuring sustained system function.

Conceptual and empirical work on the resilience of gravel barriers extends across various spatio-temporal scales (Carter et al., 1987; Orford et al., 1995a). The long term (millennial to centennial) persistence of gravel barriers is regulated by sediment supply, relative sea level rise and geological framework (Curray, 1964; Orford et al., 1996; Orford et al., 1995b). These conditions determine whether (or not) a barrier migrates landwards (transgressive behaviour), seawards (regressive behaviour), or remains stationary and builds *in situ*. Over geological time, individual barriers can exhibit more than one of these modes.

With gradual sea level rise and sufficient sediment supply, the landward (and upward) migration of the shoreface (Cattaneo and Steel, 2003) allows barriers to show long-term persistence. Gravel barriers have been observed to respond to multi-decadal sea level rise through landward migration whilst maintaining their essential form (Orford et al., 1995a). This behaviour has also been captured through various barrier modelling studies (Lorenzo-Trueba and Ashton, 2014; Nienhuis and Ashton, 2016; Nienhuis and Lorenzo-Trueba, 2019; Stolper et al., 2005).

However, barriers worldwide over the last few thousand years, under the postglacial transgression, have typically been characterised by transgressive behaviour and barrier narrowing (e.g. Leatherman, 1983). Carter et al. (1987) suggested that as sediment supply declines, gravel barriers transition from drift- to swash-aligned landforms, typically lower in elevation and with increased vulnerability to overwash, breaching and, ultimately, barrier breakdown. When the barrier width approaches the extent of storm-driven overwash further shoreface erosion leads to the long-term landward 'rollover' of the barrier landform itself (e.g. Swift et al., 1991).

High rates of sea level rise, sediment starvation (from both offshore or alongshore source areas or both) and undulating seafloor topographies can cause barriers to founder or drown in situ (Swift and Moslow (1982); Murray and Moore (2018); Emery et al. (2019), cover this range of controls), as the shoreface translates to a new landward position in a process described as 'overstepping' (e.g. Rampino and Sanders, 1980). Gravel barrier systems have greater morphological resilience to rising sea levels which must be overcome for the barrier to retreat through rollover (Forbes et al., 1995; Orford, 2011; Orford and Anthony, 2011). As a result, gravel barriers are more likely to retreat by overstepping when compared to sand-dominated ones (Mellett et al., 2012; Mellett and Plater, 2018).

Imposed atop the baseline sea level, it is infrequent storm events that drive landward migration of these landforms (Forbes et al., 1991; Hartstein and Dickinson, 2000; Orford et al., 1991a; Rodriguez et al., 2018). Although gravel barriers may exhibit considerable resistance to change under low to moderate energy conditions, threshold exceeding extreme events (acting over hours to days) may expend sufficient energy to induce system state transitions (Phillips, 2014; Phillips, 2009). Analogous to the general discussion of stability domains (e.g. Stallins, 2005), Carter and Orford (1993) proposed that barrier islands may occupy one of two alternative stable states: i) crest build-up through overtopping, resulting in stable barrier position, versus ii) crest lowering which results from barrier overwashing and retreat. During calm conditions and moderate storm events, overtopping dominates, resulting in increased crest height and a steeper and narrower barrier. This heightened and steepened barrier is more vulnerable to overwashing since the acute seaward slope encourages increased run-up by reducing the opportunity for swash percolation (Orford et al., 1995a, 1995b). Additionally, the narrower cross-section reduces the barrier's ability to resist morphological change (Leatherman, 1979). Consequently with the occurrence of a threshold exceeding storm, state transition occurs and the barrier experiences overwash and landward retreat (Forbes et al., 1995). Rather than being an irreversible state change, oscillation between the two alternative stable states represents a resilient response to extreme event forcing (Orford and Anthony, 2011).

Notwithstanding this prior research, there remain several aspects of gravel barrier resilience that have, to date, received relatively little attention:

i. Firstly, landscape-scale resilience is often difficult to predict, owing to spatial heterogeneity at the sub-landform scale (Kombiadou et al., 2019). In the context of barrier systems, landform refers to the entire alongshore and cross-shore extent of the barrier beach, dune, and back-barrier system, while sub-landform refers to one of these environments, or a cross-section through them. With some notable exceptions (Brown et al., 2019; Orford and Anthony, 2013; Stéphan et al., 2018), few studies have explored the possibility of distinct resilience trajectories within a given gravel barrier landform.
ii. For over three decades, there has been a strong recognition of the interdependencies between humans and geomorphology (Church, 2010; Haff, 2003; Hooke, 2000; Lane, 2017; Phillips, 1991; Werner and McNamara, 2007). In one recent example, Chaffin et al. (2018, 228) identify a need for research that recognises 'the complex, often nonlinear processes of individual and collective human agency that can drive regime shifts and threshold dynamics in socio-ecological systems'. Barrier systems are excellent exemplars of socio-

Table 1
Elements of resilience in gravel barrier systems.

Resilience element	Definition
Resistance	Physical resistance of landforms or capacity to absorb disturbance-induced change.
Susceptibility to state change	Likelihood of transition among qualitatively different system configurations.
Persistence	Ability to maintain long-term form despite experiencing short-term disturbances.
Function	Ability to provide erosion and flood risk reduction functions, to the benefit of nearby communities and constituent/landward ecosystems.

Definitions adapted from Long et al. (2006), Naylor et al. (2017), Orford et al. (2003), Phillips and Van Dyke (2016).

ecological systems, and frequently managed by humans to promote particular functions.

This paper investigates the role of socio-ecological modifications of gravel barrier systems and related alongshore morphological variability (barrier crest elevation, seaward slope, and cross-sectional area) in determining future gravel barrier response to storm surge with sea level rise. A numerical modelling approach was used since it enables simulation of plausible future hydrodynamic forcing conditions that deviate from the observational record, thus revealing how gravel barrier systems may behave under future environmental conditions.

2. Regional setting

The Blakeney Point Barrier System (BPBS) is a mixed sand and gravel barrier-spit (Jennings and Shulmeister, 2002) located on the North Norfolk coast, UK (Fig. 1a–c). Along its proximal section, the barrier is backed by brackish, freshwater and grazing marsh, the product of successive land reclamation schemes from the seventeenth century (Cozens-Hardy, 1927; Hooton, 1996). Towards the distal end, the back-barrier environment is characterised by the intertidal saltmarshes and mudflats and subtidal channel of Blakeney Harbour. The terminus of the BPBS, known as Blakeney Point, is characterised by an extensive aeolian dunefield (Fig. 1c).

The North Norfolk coast experiences a macro-tidal, semi-diurnal tidal regime with mean spring tidal range falling from 6.40 m at Hunstanton to 4.70 m at Cromer (Brooks et al., 2017). Over the period November 2006 to November 2009, a nearshore wave buoy installed in 7.00 m water depth at Cley-next-the-Sea (hereafter Cley) recorded annual mean significant wave heights of 0.55–0.72 m (Environment Agency, 2014; Spencer et al., 2020). Despite the prevailing low to moderate energy wind / wave climate, the North Norfolk coast is vulnerable to infrequent extreme hydrodynamic conditions. In the period 1883–2020 twenty-three surge events have been identified as having substantial local societal impacts (Table 2; Brooks et al., 2016; Haigh et al., 2017). Along the BPBS, the morphological impacts of these events range from relatively minor (e.g. the western terminus appears highly resistant to morphological changes (Barfoot and Tucker, 1980; White, 1979)), to barrier washover deposition (Clymo, 1967; Orford et al., 2003; White, 1979), and barrier breaching. There is a record of breaching following the surge events in 1897, 1938, 1949, 1953, 1978 and 2013 (Brooks et al., 2016; Orford et al., 2003); it is not known if breaching was also associated with other surge events in the period after 1883. On 5 December 2013, the BPBS experienced its most severe storm surge event since the 1953 North Sea surge. The 1953 event was, and remains, perhaps the greatest north west European environmental catastrophe of the post-World War II period, with extensive sea defence failures, widespread flooding, and considerable economic damages and fatalities along southern North Sea coastlines (McRobie et al., 2005; Pollard, 1978). The 2013 event caused washover deposition, barrier breaching in two locations, and extensive flooding along the North Norfolk coast (Andrews, 2019; Brooks et al., 2016; Spencer et al., 2015).

According to the most recent management interventions, the BPBS can be broadly divided into two sections (Fig. 1c). To the east of Cley, the barrier was actively re-profiled from the 1950s to maintain the crest height at 8 to 9 m Ordnance Datum Newlyn (ODN, where 0.0 m ODN

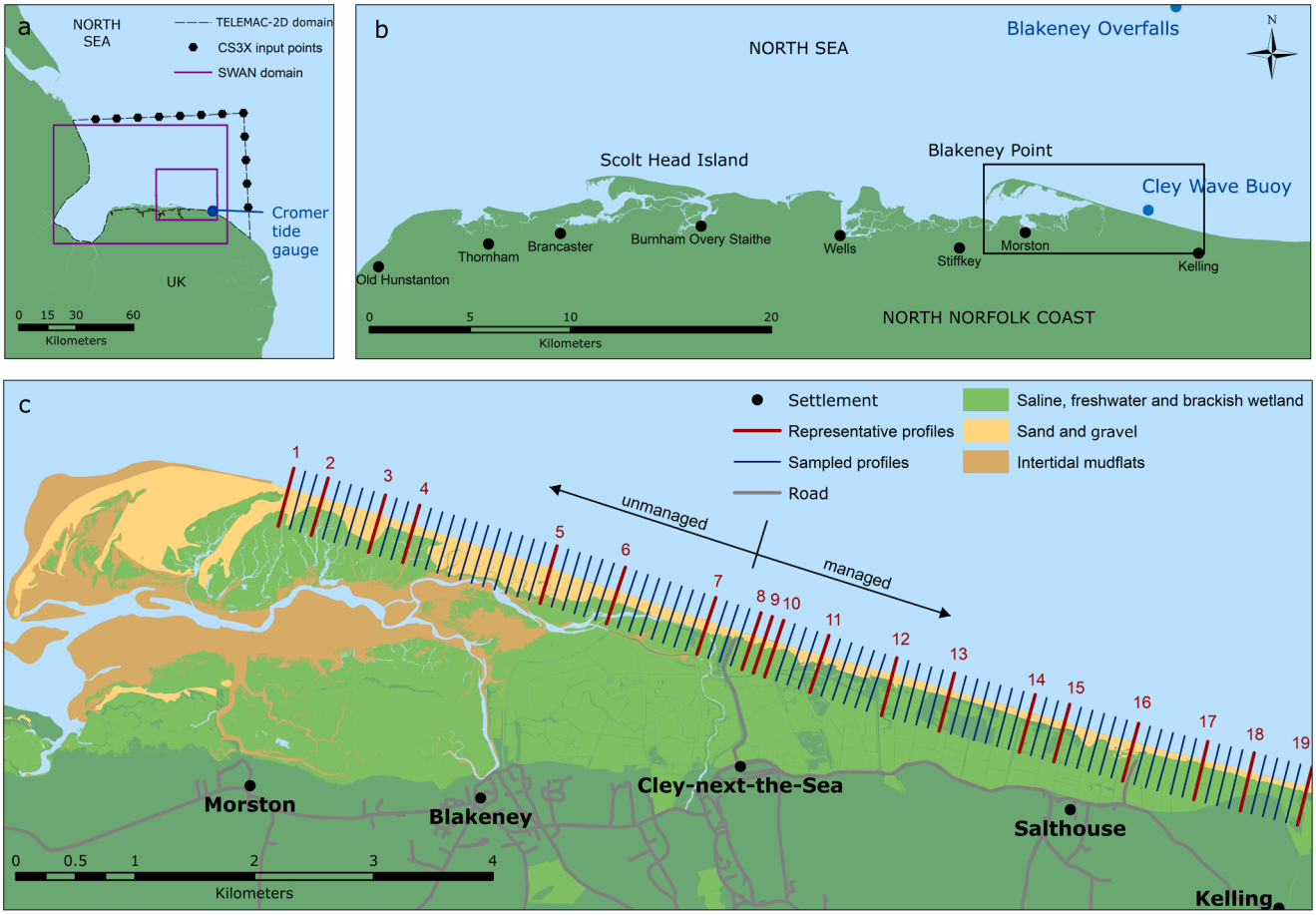

Fig. 1. Regional site map. a: the UK east coast and southern North Sea Basin, showing the TELEMAC-2D and SWAN model domains and the CS3X input points, b: the North Norfolk coast, showing wave buoys and settlements, and c: the Blakeney Point Barrier System showing settlements, road infrastructure, and coastal habitats. Ninety sampled cross-shore profiles are shown with nineteen representative profiles highlighted and numbered (see Materials and Methods section).

Table 2
Major storms on the North Norfolk coast, 1883–2021 with (where known) location-specific maximum water levels, still water level return period estimates from regional tide gauges and records of impacts and infrastructural damage.

Date	Maximum water level (locations in parentheses; key below table)	Return Period (a1)	Return Period (a2)	Return Period (a3)	Return Period (b1)	Reported Impacts and Infrastructural Damage
11/03/1883	5.49? (5) benchmark not clear					Major flooding at Wells, including quay, Freeman Street. Tramways and earthworks damaged
28/11/1897[a]	4.96 (8); 4.49? (5)					Major coastal flood event; properties flooded at Cley
26/08/1912	4.66 (6)					Possibly riverine flash flood rather than storm surge but reported for Cromer on 25/08
12/02/1938[a]	Not available					Main coast road flooded at Salthouse. Scolt Head Island suffered erosion; some dunes shortened
08/01/1949	Not available					
01/03/1949[a]	Not available					Flooding at Brancaster Staithe and Salthouse
31/01/1953[a]	5.49 (1); 5.15 (5; mean level); 5.13 (5; mean level); 4.57 (6; mean level); 6.07 (8; mean level)	21				Regional disaster. Extensive breaching of sea defences and widespread coastal flooding
20/03/1961	Not available					
16/02/1962	Not available					
29/09/1969	4.43 (3); 4.27 (5)	43		39		
02/01/1976	4.35 (3); 4.46 (5); 4.55 tide gauge	21		33		Flooding at Cley, Salthouse
11/01/1978[a]	4.62 (3); 5.51 (4); 4.91 (5); 5.55 (6); 5.26 (7); 4.90 (8); 5.14 (9)	27		7		Flooding at Holme, Wells, Cley and Salthouse. Major sea defence breach, Wells Harbour Channel
12/12/1990	4.55 (3); 4.67 (4)					Properties flooded along North Norfolk coast
20/02/1993	4.45? (2); 4.41 (5)		9	27		Flooding at Wells and Cley. Overtopping of gravel barrier at Cley and flooding of freshwater marshes
01/01/1995	4.55 (3); 4.54 (4); 4.45 (6); 4.66 (8)		6	7		
19/02/1996	Not available					Overtopping of gravel barrier at Cley and flooding of freshwater marshes for 14 days
14/12/2003	Not available					Overtopping of gravel barrier at Cley and freshwater marsh flooding
01/11/2006	4.0 (Scolt Head Island)				13	Overtopping of gravel barrier at Cley and freshwater marsh flooding
17/03/2007	3.35 (9)					Flooding at Brancaster Staithe, Wells and Blakeney. Coast road flooding
08/11/2007[a]	4.31 (1); 4.48 (2); 4.28 (3); 4.44 (4); 4.79 (5); 4.30 (6); 4.41 (7); 4.63 (8)			19		Described as a 'near miss' major storm surge
05/12/2013[a]	5.64 (1); 5.44 (2); 5.45 (3); 5.52 (4); 5.31 (5); 5.34 (6); 5.24 (7); 6.30 (8); 5.14 (9); 5.02 (10)	787		188		Major regional event. Flooding at Wells, Blakeney, Cley and Salthouse. Gravel barrier at Cley breached. Arable land at Burnham Deepdale flooded.
14/01/2016	Not available					Gale-force north-westerly winds caused an 80 cm surge. This caused seawater to come over these shingle ridge at Salthouse, causing flooding on both the Salthouse and Cley Beach roads
13/01/2017	4.31 (1); 4.13 (2); 4.10 (3); 4.13 (4); 4.43 (5); 4.63 (6); 4.27 (7); 4.50 (8); 3.84 (9); 4.12 (10)					Quay flooded at Wells, Blakeney. Overtopping of gravel barrier at Cley and flooding of freshwater marshes. 15 properties evacuated at Salthouse. Coast road closed east of Cley for 5 days.

Locations on the North Norfolk coast (see Fig. 1): (1) Thornham; (2) Brancaster Staithe; (3) Burnham Deepdale; (4) Burnham Overy Staithe; (5) Wells Harbour Quay; (6) Stiffkey; (7) Morston; (8) Blakeney; (9) Cley; (10) Salthouse. Return Period (a1) = Immingham tide gauge (http:ww.surgewatch.org); Return Period (a2) = Cromer tide gauge (http:ww.surgewatch.org); Return Period (a3) = Lowestoft tide gauge (http:ww.surgewatch.org); Return Period (b1) = North Norfolk coast (EACG (East Anglian Coastal Group), 2010).

[a] Storms highlighted in this paper.

approximates to mean sea level) (Bradbury and Orford, 2007). Barrier crest re-profiling was terminated after the winter of 2005, allowing the barrier to respond more naturally to hydrodynamic forcing conditions. To the west of Cley, the barrier has remained unmanaged at all times; it is characterised by a crest height of 5 to 6 m ODN (Bradbury and Orford, 2007).

The UK east coast is experiencing sea level rise at an accelerating rate. Using the Lowestoft tide gauge, Wahl et al. (2013) calculated a relative sea level rise (incorporating isostatic changes) of 2.7 ± 0.4 mm a^{-1} over the period 1950–2011, accelerating to 3.6 ± 0.5 mm a^{-1} (1980–2011), and 4.4 ± 1.1 mm a^{-1} (1993–2011). The latest (2018) UK Climate Projections (UKCP18) provide low, mid, and high range scenarios based on the Intergovernmental Panel on Climate Change (IPCC) Representative Concentration Pathways (RCPs), RCP2.6, RCP4.5, and RCP8.5 respectively (Gohar et al., 2018; Palmer et al., 2018). The UKCP18 Projections suggest the North Norfolk coast will likely experience a greater rate of sea level rise in the twenty-first century than it did in the twentieth century.

3. Materials and methods

3.1. Cross-sectional profile selection

Airborne LiDAR elevation models surveyed on 28 January 2013 were used to obtain pre-storm barrier morphology landward of 0 m ODN (a linear extrapolation was used to extend profiles to an optimal offshore depth of approximately 20 m), and to create the model transects with grid resolution of 3 m offshore gradually increasing to 0.5 m at the shoreline (Fig. 1c). The BPBS was sampled alongshore every 100 m, resulting in ninety cross-shore profiles (grey lines, Fig. 1c). To limit the total number of XBeach-G model runs required, a series of representative profiles was selected from the ninety sampled profiles. The seaward beach slope and the crest height were determined for each sampled profile and grouped into 1 m crest heights and 2.5-degree beach slope intervals in both the managed and unmanaged sections. A representative profile from each combination of features was then selected, ensuring that the alongshore and cross-shore variability at the BPBS was adequately represented. Seaward beach slope was calculated at 0.25 m either side of the point where the Mean High Water Line (MHWL) intersects each profile. Additionally the cross-sectional area above the Mean High Water Spring was calculated for each profile as a proxy for profile inertia, which has been defined at the landform scale as barrier cross-sectional volume (Orford et al., 1995a, 1995b). In total, eighteen profiles were extracted for future scenario modelling, seven from the unmanaged section, and eleven from the managed section. Profiles were grouped, by management regime, and then according to ranges of crest elevation, slope, and cross-sectional area (Table 3).

3.2. Numerical model chain set-up

The model chain developed by Jäger et al. (2018) for the North Norfolk coast was adapted to simulate the hydrodynamic and morphological impacts of the December 2013 storm surge at the BPBS under a selection of sea level scenarios. Water levels were modelled using TELEMAC-2D (v7p1r0) (Hervouet, 2000), then waves and nearshore water level conditions were modelled using SWAN (v41.20) (Booij et al., 1996), which informed XBeach-G, a 1D, coupled hydrodynamic and morphodynamic model for investigating extreme event impacts on gravel barriers (McCall et al., 2015; McCall et al., 2014).

The TELEMAC-2D model was driven by storm surge water levels from the UK National Oceanography Centre (NOC) CS3X tidal surge model at hourly timesteps. The UK Met Office Numerical Weather Prediction model was used to determine a temporally and spatially variable wind field during the storm surge. Offshore bathymetry was obtained from the UK Hydrographic Office (UK Hydrographic Office, 2018) and combined with coastal zone topography data (Channel Coastal Observatory, 2018; DEFRA, 2018) to produce a combined topographic-bathymetric surface for the southern North Sea. Wave conditions were modelled using nested SWAN models, forced by wave spectra from the Met Office WaveWatch III North Atlantic European model. The SWAN wind field was determined using the UK Met Office Numerical Weather Prediction model.

Observational water level data was only partially available for the period surrounding the December 2013 storm surge owing to damage to the nearest tide gauge (Cromer) during the event itself. Furthermore, no nearshore wave data was available covering this period. Accordingly, the TELEMAC-2D and SWAN models were calibrated using observational wave and water level data collected during the 8–11 November 2007 storm surge, and then validated using the more limited December 2013 data. Hydrodynamic similarities between the November 2007 and December 2013 events confer confidence in the calibration undertaken (Brooks et al., 2016). For instance, the November 2007 and December 2013 events were characterised by maximum wave height and direction of 3.5 m and 004°, and 3.8 m and 338° respectively. The maximum surge residual was also similar with 1.67 m and 1.97 m recorded at Immingham tide gauge (with the failure of the Cromer tide gauge, the nearest station in the UK National Tide Gauge Network (ntslf.org) to operate successfully during the December 2013 event) in November 2007 and December 2013 respectively.

Best fit to the observational data was obtained in TELEMAC-2D using the Nikuradse law of bottom friction and a friction coefficient of 0.0125 (RMSE values of 0.34 m and 0.16 m at Cromer tide gauge and Cley wave buoy respectively), and default parameter values in SWAN (RMSE values of 0.21 m and 0.18 m at Blakeney Overfalls (10 km offshore, 18 m water depth, Fig. 1b) and Cley wave buoys respectively). The TELEMAC-2D and SWAN models were run for the December 2013 event to validate the model performance. Both models demonstrated good agreement with observed water levels (RMSE = 0.23 m), wave height (RMSE = 0.30 m) and wave period (RMSE = 2.5 s). The reader is referred to Pollard et al. (2021) for further details of the TELEMAC-2D and SWAN calibration procedure.

XBeach-G was used to propagate water level and wave conditions onshore, and to model the resulting gravel barrier morphological response. XBeach-G was selected for this modelling study because it represents the best available modelling framework for mixed sand-gravel and pure gravel barrier environments. XBeach-G includes several hydrodynamic and morphological process that are crucial to accurately represent gravel barrier dynamics. Firstly, XBeach-G includes

Table 3
Representative profile grouping by management regime, profile crest height, slope and cross-sectional area.

Profile group	Representative profile IDs	Management regime	Crest elevation	Slope	Cross-sectional area
A	1, 5, 6, 7	Unmanaged	Low	Low-Moderate	High
B	2, 3, 4	Unmanaged	Low	Low-Moderate	Moderate
C	8, 9, 10, 18	Managed	Low	Variable	Variable
D	13, 15, 16, 19	Managed	Moderate	Moderate-High	Low-Moderate
E	12, 14, 17	Managed	High	Moderate-High	Low-Moderate

Crest elevation classified as low (<6.5 m ODN), moderate (6.5–8.0 m ODN), and high (>8 m ODN). Slope classified as low angle (<20 degrees), moderate (20–25 degrees), and high angle (>25 degrees). Cross-sectional area was classified as low (<90 m^2), moderate (90–120 m^2) and high (>120 m^2). Variable is used where profiles span low to high classifications. For representative profile ID locations see Fig. 1c.

a non-hydrostatic pressure correction term which enables individual waves to be resolved. This ensures that the processes of wave transformation, set-up, run-up, and overtopping can be modelled (McCall et al., 2014). The non-hydrostatic mode is capable of resolving infragravity waves in the nearshore which are especially important during storm conditions. Secondly, XBeach-G includes a groundwater model to account for infiltration and exfiltration effects. Infiltration has been established as a fundamental control on gravel beach morphodynamics, particularly in determining their relatively steep energy reflective form (Wright and Short, 1984). The hydrodynamics and morphodynamics of XBeach-G have been validated against a large scale flume experiment (Masselink et al., 2016; Williams et al., 2012), in addition to in-situ and remotely-sensed datasets that have captured gravel barrier storm response on the UK's south coast (McCall et al., 2015; McCall et al., 2014).

The use of XBeach-G, and consequent focus on cross-shore sediment transport processes, is further justified by characteristics of the BPBS system itself, and existing literature on extreme event impacts. The management interventions described in the Regional Setting section were achieved by bulldozing beach material landwards with mechanical plant, moving the finer fraction of material from the lower beach to the beach crest, resulting in a poorly sorted mix of coarse and fine sediments. With additional compaction from the mechanical plant, the end product was a cohesive matrix able to maintain a near vertical beach slope (Bradbury and Orford, 2007). The scale of these artificial interventions thus over-ride any alongshore variations in sediment characteristics that might result from longshore sediment transport processes.

Furthermore, Orford and Anthony (2011) observed that long-term (multi-annual to centennial) gravel barrier change is principally controlled by extreme events, sediment supply and sea level rise rate but that sediment supply can be discounted 'under conditions of limited longshore sediment supply (essentially swash-aligned, single beach-ridge barrier systems)' (Orford and Anthony, 2011, 43). Evidence of the BPBS displaying swash-aligned behaviour is provided by Pollard et al. (2020) whose historical shoreline change analysis of the BPBS showed that the classic drift-aligned signal of downdrift westward barrier extension (evident from 1886 to 2016) was replaced in the period 1981–2016 by a shift towards a more swash-aligned system, characterised by no clear alongshore variation in the rate of shoreline change (see Fig. 3, (Pollard et al., 2020)). We conclude, therefore, that our focus on cross-shore profile change is justified in the context of the contemporary behaviour of this barrier system.

The morphological outputs of XBeach-G model were calibrated and validated over the period 5 December 2013 13:00:00 to 6 December 2013 04:20:00, encompassing the storm surge event. Model calibration was achieved through systemic variation of the infiltration coefficient (kx, in the range 0.001, 0.01, 0.1, 0.2, 0.3, 0.4, 0.5, 0.6, 0.7) and the Manning bed friction coefficient (bfc, in the range 0.02, 0.024, 0.028, 0.032, 0.034). XBeach-G was run with grain size D_{50} and D_{90} values of 0.019 m and 0.035 m calculated from particle size analysis at the study site just to the west of representative profile 16. Model skill was assessed by calculating the Brier Skill Score (BSS, Sutherland et al. (2004)) and crest elevation difference between the post-surge model output and post-surge LiDAR elevation surveys collected on 3 February 2014. Each calibration run was then ranked on both the BSS and crest height difference. Ranks from each measure were multiplied together (applying an equal weighting to BSS and crest height performance) to obtain an overall rank for each calibration parameter combination (Pollard et al., 2021). Best performance across all the validation cases was achieved using infiltration and bed friction coefficient values of 0.4 and 0.02 respectively.

XBeach-G reproduced observed morphological change on profiles that underwent minimal change, washover, and sluicing washover, but performed less well where profiles underwent barrier crest accretion (here the model underestimated accretion (Pollard et al., 2021)). The model was unable to reproduce barrier breaching leading to the omission of profile 11 which coincided with a breach location. The inability to simulate breaching impacts derives from XBeach-G being a one-dimensional model developed to investigate cross-shore sediment transport during extreme events. Effectively modelling breaching dynamics would require a two-dimensional model framework (Stripling et al., 2008).

3.3. Numerical model chain application

The model chain was initially run for the December 2013 event, without any additional sea level rise, and then for a range of future sea level scenarios produced by UKCP18 (Palmer et al., 2018). Following Hinkel et al. (2014), the range of future sea level scenarios was represented using the 5th percentile from RCP2.6 projected to 2050, the 50th percentile from RCP4.5, and the 95th percentile from RCP8.5, both projected to 2100. Accordingly, future sea level rise values of 0.17 m (low), 0.55 m (moderate), and 1.13 m (high) respectively were used. Future sea level conditions were propagated through the model chain from the TELEMAC-2D model, through the nested SWAN grids, to the XBeach-G model. Each profile was run ten times, with random statistical seeding of the wave time series for each run to avoid results unique to a given set of wave conditions (McCall et al., 2014). This approach was repeated for the December 2013 event and the three future sea level scenarios, giving a total of 720 model runs.

There remains considerable uncertainty regarding the direction and magnitude of future changes to storm surge and wave conditions (Grabemann et al., 2015; Woth et al., 2006). The most recent synthesis of this work is provided by the UKCP18 Marine Report which finds that the direction and magnitude of future changes to storm surge and wave heights remains uncertain, with no agreement in the sign of change among model projections (Palmer et al., 2018). Specifically, UKCP18 states 'increased future flood risk will be dominated by the effects of time-mean sea level rise, rather than changes in atmospheric storminess associated with extreme coastal sea level events' (Palmer et al., 2018, 3), supporting the UK's Marine Climate Change Impacts Partnership (MCCIP) Science Review that 'observational evidence shows that patterns in extreme sea levels are controlled by changes to mean sea level, rather than changes in storminess' (Horsburgh and Lowe, 2013, 27). A recent modelling study by Vousdoukas et al. (2017) shows that, in a relatively extreme sea level rise scenario (98 cm of relative sea level rise by 2100 under RCP8.5), 20% of the total rise in the North Sea as a whole might be explained by changes in storm surge and wave climate, although with this contribution decreasing as sea level rise accelerates towards the end of the period. However, in the underlying analysis dataset, the relative change in storm surge levels showed an increase eastwards across the North Sea, where 'most of the UK east coast showed small decrease or no change' (Vousdoukas et al., 2016, 3180). For future UK wave climates, 'high resolution wave simulations suggest that the changes in wave climate over the 21st century on exposed coasts will be dominated by the large-scale response to climate change. However, more sheltered coastal regions are likely to remain dominated by local weather variability' (Palmer et al., 2018, 4). Accordingly, no increase of storm surge or wave heights was included in this modelling exercise.

4. Results

Compared to a scenario of no sea level rise, when forced with future sea level scenarios, TELEMAC-2D modelled water levels increased proportionally relative to the input scenario. Propagating the modelled water level increase to the SWAN model resulted in an increase in significant wave height, particularly during low tide (Fig. 2). This is because at low tide the sea level driven rise in water level permits larger waves to form, whereas at the peak of the surge water levels are already sufficiently high such that further increases in water level due to sea level rise have a limited effect. Standard deviation in significant wave

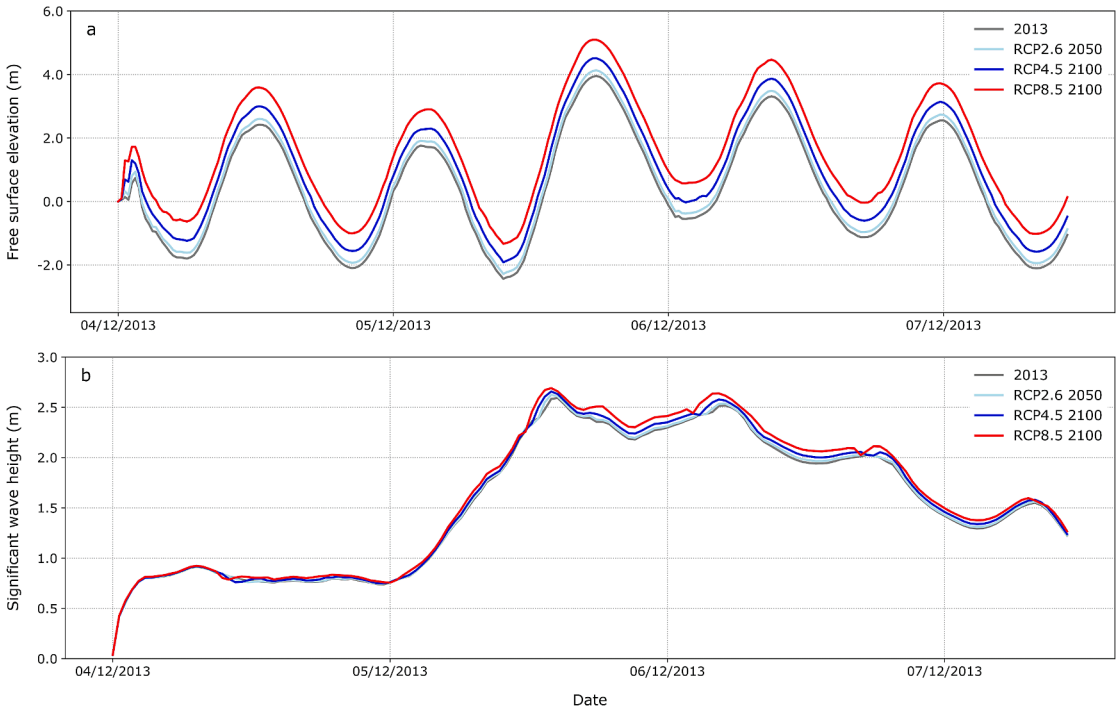

Fig. 2. Historic and future water levels and wave characteristics for the period 4 December 2013 15:00:00 to 7 December 2013 12:00:00: (a) significant water levels at Cromer; (b) significant wave height at Cley (for locations see Fig. 1).

height, measured at the Cley wave buoy (Fig. 1b, 400 m offshore, 7 m water depth) was 0.65 m, 0.66 m, 0.67 m, and 0.69 m during the December 2013 storm surge under no, low, moderate, and high sea level rise scenarios respectively.

Fig. 3 displays the morphological and hydrodynamic impact of storm surge conditions on the grouped representative profiles under no, low, moderate, and high sea level rise scenarios. Figs. 4 and 5 capture the range of morphological changes and associated landward overtopping volume (volume of water per unit width over the modelled time period) in response to storm surge and future sea level rise scenarios. The morphological change from a single model run is presented, alongside the distribution in landward overtopping volume from all ten model runs (for each profile and scenario). Variation in landward overtopping volume arises from differences in wave conditions and resultant morphological change.

Groups A and B derived from the western unmanaged section of the BPBS and are characterised by low crest elevations (<6.5 m ODN) and low-moderate seaward slopes (<25 degrees). The two groups are distinguished by their barrier cross-sectional areas, with Group A displaying relatively higher cross-sectional area (>120 m^2) and Group B relatively lower cross-sectional area (90–120 m^2) (Table 3).

Groups A and B displayed either crest stability or limited (<1 m) crest lowering under no and low sea level rise scenarios, along with some landward movement of the barrier crest, generally 2 to 6 m (Fig. 3b). Under moderate and high sea level rise, there was greater separation between the two groupings. Group A continued to display limited crest lowering, with the barrier crest retreating landwards on average around 8 m under the moderate and high sea level rise scenarios respectively. Under the same conditions, Group B exhibited an approximate doubling in crest lowering (Fig. 3a). The crest elevation reductions experienced by Group B under moderate and high sea level rise scenarios resulted in post-surge crest heights of around 4 m (Fig. 4c). Group B also experienced mean landward movement of the barrier crest, of just below 10 m under the high sea level rise scenario.

The morphological changes experienced by each group had implications for landward overtopping volume (Fig. 3c). For Group A, landward overtopping volume increased steadily from the no to high sea level rise scenarios (Fig. 4a, b). For Group B, the greater reductions in crest elevation under moderate and high sea level rise scenarios were accompanied by greater increases in landward overtopping volume (Fig. 4c, d).

Groups C, D, and E derived from the eastern managed section of the BPBS and were characterised by diverse morphologies (Table 3). Group C profiles had low crest elevations (<6.5 m ODN) and variable seaward slopes and barrier cross-sectional areas. Groups D and E were both characterised by moderate-high seaward slopes and low-moderate barrier cross-sectional area but were distinguished by crest elevation; Group D exhibited moderate pre-surge elevations (6.5–8 m ODN) while Group E profiles had high pre-surge elevations (>8 m ODN).

The high variability in the initial morphology of profiles from Group C was reflected in highly variable morphological and hydrodynamic responses to storm surge conditions, regardless of sea level rise scenario. Modelled mean crest elevation change remained relatively consistent across all sea level rise scenarios, with a mean reduction of between 0.5 and 1 m (Fig. 3a). For all sea level rise scenarios, this resulted in post-surge crest elevations of around 4 m ODN. Mean crest positional change was highest of all the profile groupings with 6 to 8 m of landward retreat, even under no and low sea level rise. Under moderate and high sea level rise, landward retreat ranged between 8 and 10 m (Fig. 3b). Group C was characterised by relatively high mean landward overtopping volumes under no and low sea level rise scenarios, increasing steadily under the moderate and high scenarios.

Group D experienced considerable reductions in crest elevation regardless of the sea level rise scenario. In all cases a mean reduction of >2.5 m was modelled (Fig. 3a). However, owing to greater pre-surge crest heights, post-surge crest elevations typically remained above 4.20 m ODN. This corresponds with the storm surge peak still water level of 4.20 m (upon which wave driven run-up and any increases in sea level are superimposed). Mean total landward overtopping volume was among the highest of all profile groupings, regardless of the scenario. Landward crest movement was moderate for these profiles, with mean values ranging between 2 and 4 m (Fig. 3b).

Finally, Group E underwent relatively limited crest lowering in response to scenarios of no sea level rise (Fig. 3a). Under low and

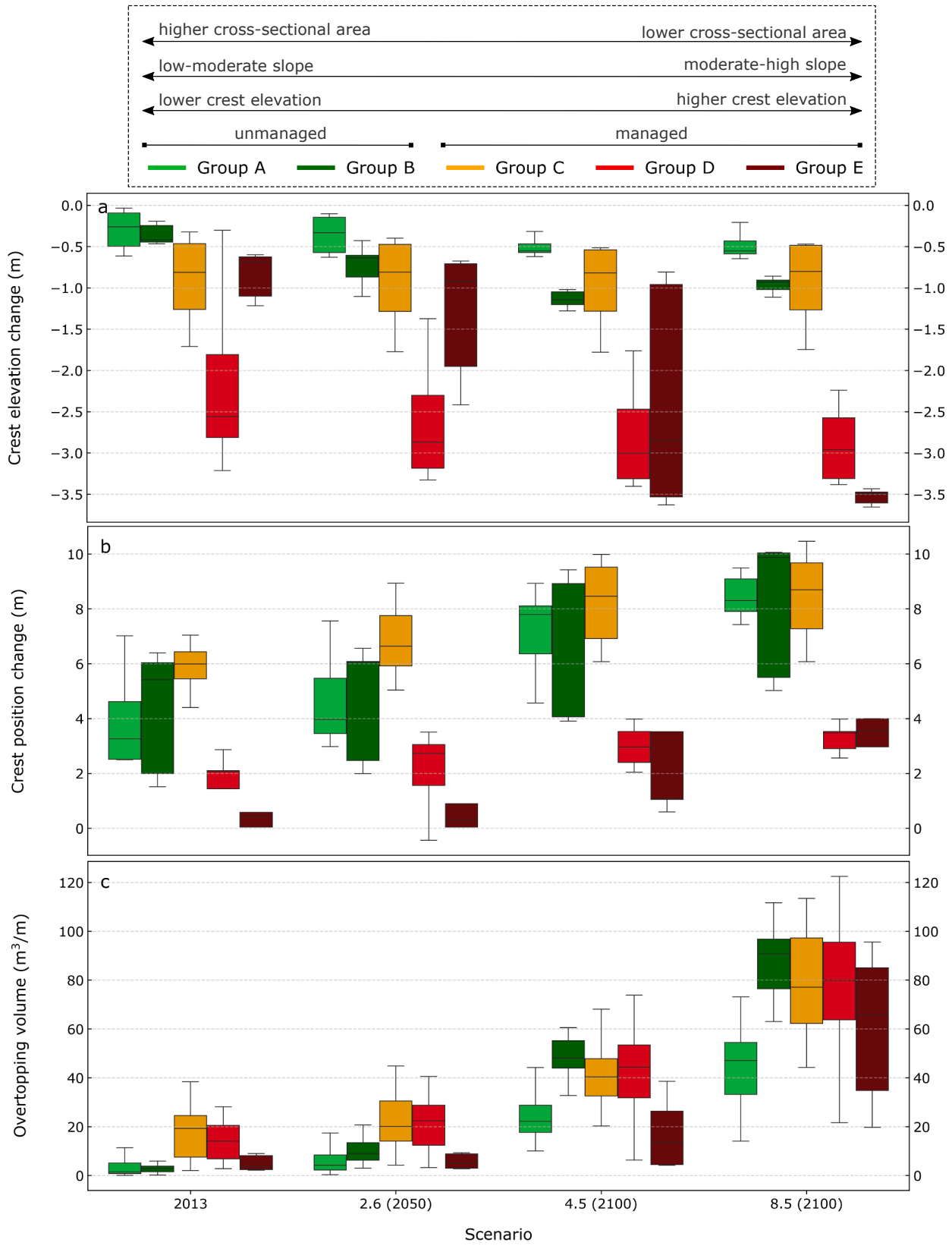

Fig. 3. Grouped profile responses to storm surge and sea level rise. A: crest elevation change, B: crest position change, C: total landward overtopping volume. Each subplot incorporates outputs from the 10 model runs performed for each profile. Profile groupings specified in Table 2.

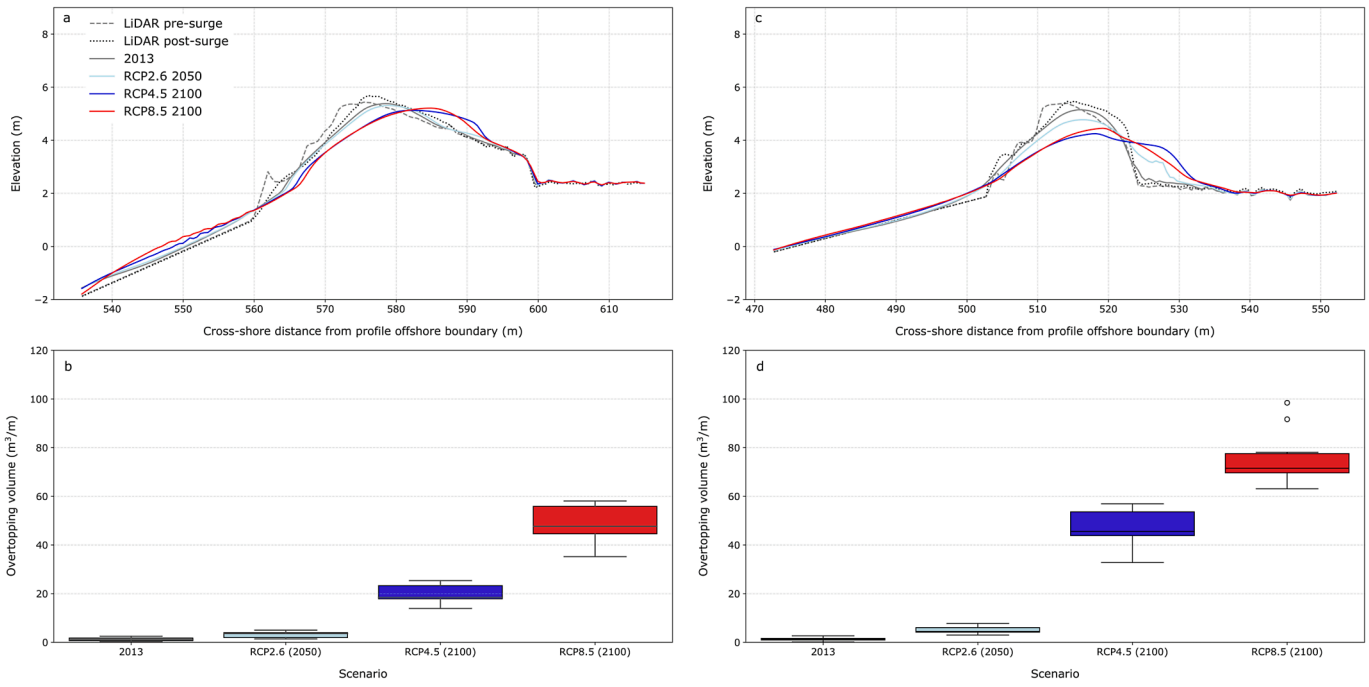

Fig. 4. Illustrative profiles of morphological change and landward overtopping volume for representative profile Groups A and B in response to a December 2013 style storm surge under three future sea level rise scenarios. Representative profiles 6 (a, b) and 2 are used (c, d) to illustrate the behaviour of Groups A, and B respectively. Both groups derive from the western unmanaged section of the BPBS.

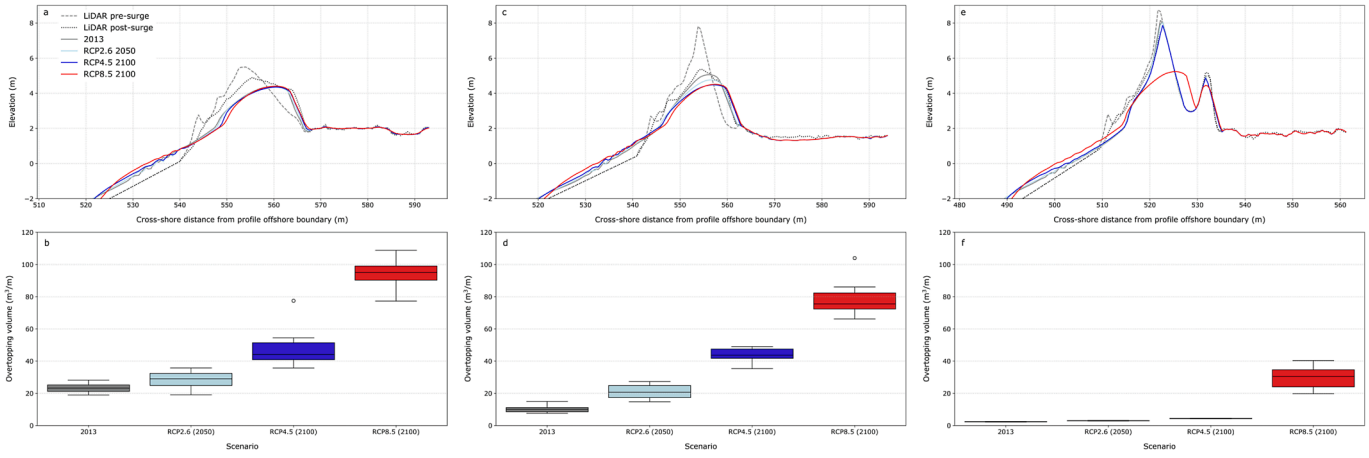

Fig. 5. Illustrative profiles of morphological change and landward overtopping volume for representative profile Groups C, D, and E in response to a December 2013 style storm surge under three future sea level rise scenarios. Representative profiles 9 (a, b), 13 (c, d), and 12 (e, f) are used to illustrate the behaviour of Groups C, D, and E respectively. All groups derive from the eastern managed section of the BPBS.

moderate sea level rise, this group exhibited a large range in crest elevation change from <1 m to >2.5 m, as some profiles experienced washover deposition while others continued to resist substantial changes. Under the high sea level rise scenario, the range of crest elevation responses contracted, as all profiles experienced crest lowering of >3 m (Fig. 3a). Group E displayed the lowest mean landward crest movement of all groups, largely because of minimal morphological change under no to low sea level rise scenarios. Under the moderate and high sea level scenarios, mean landward retreat was similar to that modelled for Group D. Mean landward overtopping volume for Group E was low under no and low sea level rise scenarios, rising slightly under moderate sea level rise, and more substantially for the high sea level rise scenario (Fig. 5e, f).

Fig. 6 shows a kernel density estimate (KDE) of total landward overtopping volume for each of the future scenarios, arranged by management regime. KDE was used to obtain an indication of the probability distribution of total landward overtopping volume, by replacing each value with a distribution derived from surrounding values. Fig. 6a illustrates that the landward overtopping volume associated with the 2013 scenario is highly uniform and rather low, peaking at ca. 0.1 m^3/m. This uniformity is maintained to some extent under the low sea level rise scenario. For the moderate sea level rise scenario, the distribution is flattened markedly, and then shifts towards higher discharge values for the high sea level rise scenario. For the managed profiles, the density distribution is spread over a greater range in mean landward overtopping volume (Fig. 6b). In all cases, the modal distribution for the managed profiles is skewed towards higher landward overtopping volume values compared to the unmanaged profiles. Visually, this results in platykurtic distributions which extend towards more extreme total landward overtopping volumes. In addition to exhibiting

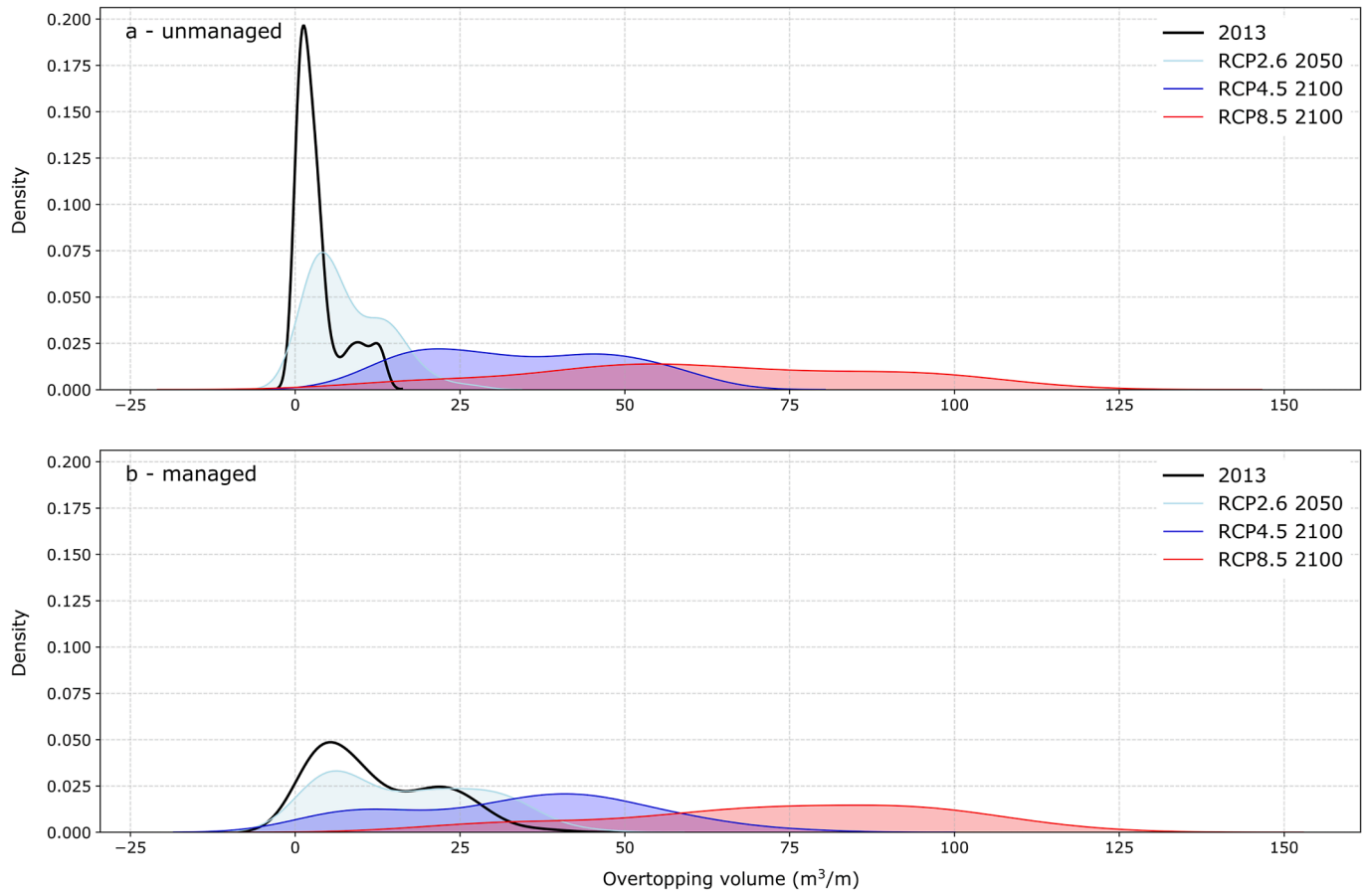

Fig. 6. Landward overtopping volume under storm surge conditions and future sea level rise. a: unmanaged profiles, b: managed profiles.

more extreme total landward overtopping volume, the managed profiles also display greater variability.

5. Discussion

5.1. Alongshore morphological variability introduces distinct episodic resilience trajectories

Alongshore heterogeneity in gravel barrier resilience may compromise continuing resilience at the landform scale (Kombiadou et al., 2019). Representative cross-shore profiles sampled along the Blakeney Point Barrier System (BPBS) reveal considerable alongshore variation in pre-surge profile morphologies, related to barrier crest elevation, seaward slope, and cross-sectional area. These morphological differences arise partly owing to the persistence of alternative management regimes along different barrier sections, and they result in a spectrum of episodic resilience trajectories at the sub-landform scale. The term "episodic resilience trajectory" is used because this study considers barrier behaviour on an "event" timescale, as a result of a surge event imposed atop a rising baseline sea level.

The morphological response of Group E demonstrates that gravel barrier sections with sufficiently high crest elevations (>8 m) can resist morphological change under storm surge conditions combined with moderate sea level rise (Fig. 5e), in line with previous studies (Masselink and Van Heteren, 2014; Sallenger, 2000). However, under high sea level rise scenarios, and where wave run-up exceeded the profile crest, profile morphological response included substantial crest lowering, landward retreat, and severe washover deposition (Fig. 3). Since Group E profiles were characterised by pre-surge elevations exceeding 8 m ODN, post-surge crest elevations remained relatively high compared to other profile groupings which also exhibited crest lowering. Consequently, for Group E profiles, the magnitude of landward overtopping volume remained lower when compared to profiles that experienced a lesser degree of crest lowering but ended with lower post-surge crest heights (compare the response of Groups C, D, and E in Fig. 5). Hence, profiles with steep, high pre-surge morphologies continue to act as a barrier to landward overtopping volume, even when overwashing occurs.

While crest elevation provided a first order control on the resilience of Group E profiles, Groups A, B, and C were all characterised by low crest elevations (<6.5 m ODN). Groups A and B also shared low-moderate seaward slopes (<25 degrees). Under no and low sea level rise scenarios, profiles from Groups A and B were characterised by crest stability / limited lowering (Fig. 4a, c). This behaviour can largely be explained by low-moderate seaward slopes which provide greater opportunity for swash percolation and resultant reduced wave run-up extents (Bujan et al., 2019; Buscombe and Masselink, 2006; Poate et al., 2013; Wright and Short, 1984).

Under moderate and high sea level rise scenarios, low-moderate seaward slopes were no longer sufficient to facilitate minimal profile change in response to storm surge conditions. Under moderate and high sea level rise conditions, Group A exhibited increased crest lowering indicative of washover deposition and associated landward rollover (Fig. 4a). The increase in baseline water level was accompanied by a corresponding increase in total landward overtopping volume (Fig. 4b). For Group A profiles, landward overtopping volume was predominantly controlled by water level, rather than being strongly moderated by morphological changes. The future functional performance of barrier sections characterised by this morphology is reasonably predictable since future landward overtopping volume can be determined through its linear relationship to sea level rise (as suggested by Orford et al. (1995b)). In contrast, Group B profiles exhibited considerable crest lowering under moderate and high sea level rise scenarios (Fig. 3a). This

resulted in post-surge crest elevations of approximately 4 m ODN (Fig. 4c). LiDAR surveys following the December 2013 event revealed that locations where the barrier breached were characterised by post-surge crest elevations of <4 m ODN. Accordingly, the crest elevation lowering modelled for the Group B profiles could be considered a breaching-style response. To confirm this assertion would require the development of a two-dimensional gravel barrier model, given the complexities associated with barrier breaching mechanisms (Bradbury, 2000; Muir Wood and Bateman, 2005). Regardless of whether lowering to 4 m ODN indicates breaching or not, the implications for landward water flows are clear, with total landward overtopping volume increasing by a more than proportionate amount relative to the increase in water level due to sea level rise (Fig. 3c). This emphasises the importance of morphological change in determining landward water flow.

Barrier cross-sectional area emerges as the primary determinant of barrier morphological response under moderate and high sea level rise scenarios. Group A profiles were characterised by high pre-surge cross-sectional area (>120 m^2) while Group B profiles were characterised by moderate cross-sectional area (90–120 m^2). On the one hand, this demonstrates that if barrier volume can be maintained, resilient responses are possible even under high future sea levels. Conversely, if sediment is lost from the system, barrier locations previously characterised by wave-dissipating low angle profiles might be vulnerable to extreme morphological change in the future, with the potential for breaching. This supports earlier work on southern England gravel barriers by Bradbury et al. (2005) and similar observations have been made at the Sillon de Talbert barrier, Channel coast, Brittany, France (Stéphan et al., 2018; Stéphan et al., 2012). There, sediment-starved sections of the barrier crest have not recovered following major erosion events in 2008 and 2013–14 (Stéphan et al., 2018). By comparison, the middle section of the barrier where sediment is relatively more abundant, recovered its pre-surge height over 3 to 4 years, through overtopping driven build-up of the barrier crest. More generally, modelling work by Brown et al. (2019) has also emphasised the importance of barrier cross-sectional area. In their research, when two barrier sections of different widths were exposed to an equivalent sea level rise of >3 mm a^{-1}, the section characterised by a greater barrier width experienced overtopping rather than overwashing, as run-up was reduced by percolation of incoming swash.

Despite sharing the low crest elevations of Groups A and B, Group C profiles exhibited variable seaward slopes and cross-sectional areas. These mixed morphological characteristics reflect the transition of parts of the barrier from morphologies that carry a clear imprint of previous management to a more natural unmanaged state. While some profiles within this group underwent relatively limited change (similar to Group A, Fig. 4a and b), others exhibited crest elevation lowering, landward retreat, and washover more similar, though not quite as extreme, as profiles from Group D (Fig. 5a and b). This explains the generally higher and more variable landward overtopping volumes that characterise the Group C profiles. Several of the Group C profiles encountered the December 2013 storm having sustained washover deposits during previous storm surge events (most notable on 8 November 2007). This resulted in lower pre-surge crest heights compared to barrier sections that had not experienced washover deposition previously (Groups D and E). It is likely that these lower pre-surge crest heights, combined with steeper foreshore slopes (a remnant of the previous interventionist management regime), resulted in the enhanced wave run-up necessary to generate further overwashing and high landward overtopping volume (Bujan et al., 2019; Poate et al., 2013; Poate et al., 2016).

The observation that Group C profiles exhibited repeated severe washover deposition suggests that several storms are required to return

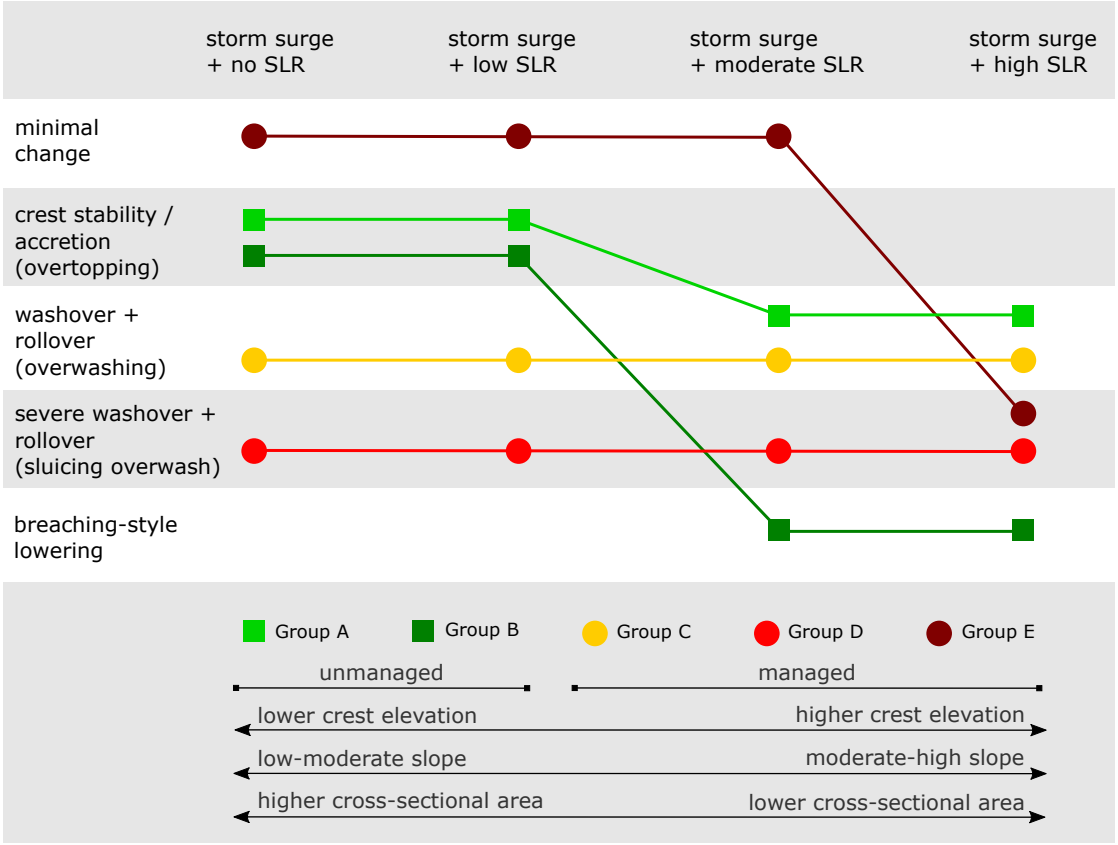

Fig. 7. Spectrum of potential BPBS gravel barrier episodic resilience trajectories. Square and circular icons are used to distinguish the unmanaged and managed barrier sections respectively. Morphological and hydrodynamic responses adapted from Orford et al. (1991b).

these profiles to a low angle, low crested form, capable of a more subdued storm response. This supports previous studies which assert that termination of interventionist management will likely be characterised by a transition period during which the barrier system relaxes towards a more natural state (Orford et al., 2018). For example, observations of management regime change at Porlock barrier, Bristol Channel UK, suggest that initial readjustment of the system can be followed by relative stability as the system approaches a more natural equilibrium with hydrodynamic forcing conditions (Hudson and Baily, 2018; Orford et al., 2003). This study has further shown that this transitional phase can be associated with high landward water flows, since barrier crest lowering may occur prior to a reduction in seaward slope, resulting in wave run-up extents that are higher than would be expected for a low crested barrier of more natural form.

Pre-surge variations in the alongshore barrier crest elevation, seaward slope angle, and cross-sectional area give rise to a spectrum of episodic resilience trajectories under a range of sea level scenarios (Fig. 7). The modelling undertaken in this study reveals how the barrier may behave if the pre-surge morphology encounters a surge of similar magnitude to the December 2013 event, under varying sea-level scenarios. Accordingly, Fig. 7 does not necessarily capture the full range of potential episodic resilience trajectories, nor does it suggest that all of these trajectories represent long-term stable states. Recognition of this alongshore diversity assumes crucial relevance for the resolution at which such features should be monitored as they respond to changing environmental conditions. Orford et al. (2018) have noted that the BPBS is relaxing towards a more natural state in response to successive storm surge events, following the termination of active management. If this trend continues, by the time moderate to high sea level scenarios are realised, a greater portion of the barrier may be characterised by morphologies similar to Groups A, B and C, rather than D and E. In terms of future barrier resilience, this evolutionary model is encouraging since Groups A and C respond to storm surge forcing through washover formation and landward rollover. These processes ensure the conservation of barrier sediments as the barrier retreats to a more landward position. More concerning from a landform coherence perspective, however, is the episodic resilience trajectory of Group B which, through excessive crest lowering, could result in barrier breakdown if it were to persist at multiple alongshore locations.

5.2. The role of human agency in determining gravel barrier resilience

Natural barrier resilience may be deflected by the presence, and activities, of human populations. Humans introduce further complexity to coastal landscapes, both through direct intervention to their material and structural characteristics (e.g. Carter, 1988; Inman and Brush, 1973; Nordstrom, 2000; Werner and McNamara, 2007) and through assigning subjective (and often contradictory) value to the landscapes they interact with and depend on (Piégay et al., 2018). It is important to recognise that human actions can hinder the stabilizing feedbacks that allow barriers to persist as sea level rises and shorelines erode. Previous modelling studies have established that the presence of human settlement and infrastructure on barrier islands increases barrier vulnerability to drowning as sea levels rise (Lorenzo-Trueba and Ashton, 2014; Miselis and Lorenzo-Trueba, 2017; Rogers et al., 2015). Increased vulnerability to drowning arises because barriers supporting human infrastructure are unable to migrate landwards through rollover (Lazarus, 2014; McNamara and Werner, 2008).

The modelling conducted here complements these longer-term studies by investigating the impact of human intervention on barrier resilience at event timescales. Active re-profiling of the Cley-Salthouse barrier introduced systematic morphological differences between the eastern (previously managed) and western (unmanaged) sections of the BPBS. Accordingly, in a coastal defence context, the functional resilience of this landform to future storm surge and sea level rise scenarios cannot be meaningfully understood without considering the socio-ecological nature of this environment. Across both the unmanaged and managed sections, the BPBS displays considerable heterogeneity regarding the elements of resilience (resistance, susceptibility to state change, persistence, and function) considered here (Table 1). Different combinations of these elements will affect evolutionary pathways.

High resistance to change is demonstrated by several of the profile groups, but for different reasons. From the unmanaged section, Groups A and B were highly resistant to change resulting from storm surge conditions with no and low sea level rise scenarios owing to effective wave run-up dissipation. Only under moderate and high future sea level rise did these profiles undergo more extreme crest lowering and even then, it was only the Group B profiles, with lower cross-sectional area, that underwent severe morphological changes. From the managed section, Group E, representing the highest, steepest profiles, exhibited considerable resistance to change, owing to a highly reflective form and crest elevations which precluded overtopping and overwashing flows, even at the peak of the surge. Under high sea level rise scenarios, resistance gave way to dramatic state changes as these profiles experienced considerable crest lowering, landward retreat, and associated washover formation. For the remaining profiles from the managed section (Groups C and D), resistance was lower and susceptibility to state change was high, even under storm surge conditions with no additional sea level rise (Fig. 5a and c).

Barrier persistence depends on the resistance and susceptibility to state change of different barrier sections in response to storm surge conditions, in addition to alongshore sediment transport gradients. The potential for barrier persistence despite storm surge conditions was demonstrated by natural healing of barrier breaches (which occurred in the eastern managed section) within two months of the December 2013 storm surge (Spencer et al., 2015). Strong regional easterly winds were likely crucial to this healing process, though the source of sediment which filled the breaches remains unknown. Previous studies have proposed that disparate storm responses in different alongshore barrier sections may contribute to barrier breakdown (e.g. the conceptual model of Carter et al. (1987); and empirical work by Orford et al. (2002) and Penland and Ramsey (1988)). Additionally, studies focusing on the BPBS specifically have suggested that variations in cross-shore erosion rate (which is driven largely by extreme water level events such as storm surges) and the resulting alongshore variability in shoreline position introduced by such anchor points could promote barrier disintegration, hampering persistence of the BPBS (Bradbury and Orford, 2007; Environment Agency, 2010).

Despite the contemporary landform persistence indicated above, the modelling performed here reveals that under future sea level rise scenarios, the integrity of the BPBS could be threatened. As mentioned above, profiles from Group B underwent considerable crest lowering (to approximately 4 m ODN) when forced with storm surge conditions under moderate and high sea level rise (Fig. 4c). Given that this elevation lies below the storm surge still water level, barrier breaching could plausibly result in these locations. Considering that the back barrier along the western section of the BPBS is tidally influenced, there exists potential for breaches to endure through the positive feedbacks of channel deepening and scour (Davis et al., 1989). If breaching and subsequent channel formation did occur this could hamper long term persistence of the BPBS since the formation of tidal inlets can disrupt longshore sediment transport, leading to the formation of discrete sediment cells, landward migration, and barrier disintegration (Carter et al., 1987). Barrier landforms elsewhere are already experiencing an increase in migration rate most probably related to enhanced sea level rise (e.g. Odezulu et al. (2018); Rodriguez et al. (2018)) and modelling studies further intimate that such behaviour may become more widespread as sea level rise accelerates (e.g. Ashton and Lorenzo-Trueba (2018), Moore and Murray (2018)).

The coastal risk reduction function performed by gravel barriers depends fundamentally on their continued persistence at the landform scale. Landward overtopping volume, which is closely linked to

morphological change, provides an indicator of landward flooding hazard. Fig. 6 illustrates the influence of management regime on landward overtopping volume under the range of future sea level rise scenarios. The leptokurtic landward overtopping volume distribution exhibited by the unmanaged profiles in response to storm surge with no and low sea level rise scenarios reflects the consistent morphological response of these profiles (Fig. 6a). Here the total landward overtopping volume distribution is low and predictable, concentrated at values <25 m^2, representing effective functional performance. The more subdued landward overtopping volume distributions of the managed profiles reflect the morphological diversity shown by these profiles in response to extreme event forcing (Fig. 6b). Under every scenario, the managed profile distributions are characterised by a long tail which extends towards more extreme landward overtopping volumes. This is evident even for no and low sea level rise scenarios suggesting a failure in function performance of this part of the barrier is possible even without moderate to high sea level rise. Under moderate and high future sea level scenarios, landward overtopping volume distributions are similar for the unmanaged and managed profiles suggesting that the ability of the barrier to limit landward water flows may be severely limited in future.

6. Conclusions

Gravel barriers are frequently managed to ensure and enhance coastal risk reduction functions (UK: Hudson and Baily, 2018; Orford and Barry, 2016, Stripling et al., 2008; mainland Europe: Bergillos et al., 2017, Stéphan et al., 2012; New Zealand: Brown et al., 2019). Shifting perceptions concerning the extent to which humans should be modifying environmental systems, alongside funding constraints and future sea level rise projections, means that interventionist management is increasingly seen as unsustainable (Dale et al., 2017; Spalding et al., 2014). Alternative approaches towards coastal management seek to incorporate 'natural' processes and landforms into more conventional strategies; with the Dutch sand engine being an archetypal example (de Vriend et al., 2014; Kabat et al., 2009). The success of such approaches depends crucially on the performance of coastal risk reduction functions under both present and uncertain future forcing conditions (Möller, 2019).

Certain characteristics of gravel barriers are inherently resilient. For instance, coarse-grained composition typically leads to a reflective beach form which is effective at dissipating incoming wave energy during high energy storm events. The reprofiling regime at the BPBS introduced differences in barrier crest elevation, seaward slope, and cross-sectional area when compared to a more natural morphology. Exposure to previous storm surge events since the termination of reprofiling resulted in a variety of intermediate morphologies between the managed and unmanaged extremes. When modelled under storm surge conditions and future sea level rise scenarios, a spectrum of episodic resilience trajectories was revealed. This clearly illustrates the potential coexistence of multiple system states confirming the suitability of ecological definitions of resilience for describing such landscapes. Coastal landscapes are rarely morphologically uniform for large stretches. The contrasting trajectories identified here demonstrate the value in assessing coastal resilience at the sub-landform scale.

The various elements of resilience do not always align. An artificially heightened and steepened barrier may be highly effective at providing flood risk reduction despite inhibiting geomorphologically resilient responses to flood generating events. Furthermore, gravel barriers must be permitted to internally recycle sediment in order to maintain the integrity of the landform. The interaction between overtopping and overwashing facilitates a resilient barrier response to extreme hydrodynamic events since it allows barrier cross-sectional area to be conserved whilst facilitating barrier retreat, thus maintaining a constant position within the tidal frame. In addition to preventing cross-shore sediment transport, artificial re-profiling of the barrier crest increases the threshold stress which must be exceeded to transition between alternative system states. An excessively high and steep barrier crest prevents geomorphological adjustment to medium-sized events, and in doing so increases the potential for substantial geomorphic change during more extreme events.

Over decadal timescales, and considering future sea level rise acceleration, attempts to artificially maintain gravel barriers at overly seaward locations and steep, narrow profile forms will likely increase the potential for sluicing overwash and, in some cases, breaching. Coastal risk management strategies should consider allowing gravel barriers to adopt more natural morphologies even if this means that over crest water flows occur more frequently, and potentially with greater magnitude during the intermediary relaxation phase. The resultant increased predictability and reduced magnitude of erosion and flooding impacts should enable gravel barriers to be integrated to coastal risk management strategies in a way that is sustainable under present and future forcing conditions. Such insights will help to temper our expectations regarding the coastal erosion and flood risk reduction functions of gravel barriers in the face of global environmental change.

Data availability

The data used to support this article are available at PANGAEA, Data Publisher for Earth & Environmental Science (https://www.pangaea.de/).

Pollard, J.A., Christie, E.K., Spencer, T., Brooks, S.M. 2022. XBeachG Storm Surge Modelling at Blakeney Point, UK. PANGAEA, https://doi.pangaea.de/10.1594/PANGAEA.920040.

Declaration of Competing Interest

The authors declare that they have no known competing financial interests or personal relationships that could have appeared to influence the work reported in this paper.

Acknowledgements

This work was funded by the NERC/ESRC Data, Risk and Environmental Analytical Methods (DREAM) CDT, Grant/Award Number: NE/M009009/1. It is also a contribution to UKRI NERC "Physical and Biological dynamic coastal processes and their role in coastal recovery" (BLUE-coast), Grant Award Numbers: NE/NO015878/1 (Spencer), NE/N015924/1 (Brooks).

References

Andrews, J., 2019. Spit extension and barrier rollover at Blakeney Point and Salthouse: historic maps and field observations. Bull. Geol. Soc. Norfolk 69, 1–28.

Ashton, A.D., Lorenzo-Trueba, J., 2018. Morphodynamics of barrier response to sea-level rise. In: Moore, L.J., Murray, A.B. (Eds.), Barrier Dynamics and Response to Changing Climate. Springer, pp. 277–304.

Barfoot, P.J., Tucker, J.J., 1980. Geomorphological changes at Blakeney Point. Norfolk. Trans. Norfolk Norwich Nat. Soc. 25, 49–60.

Bergillos, R.J., Rodríguez-Delgado, C., Ortega-Sánchez, M., 2017. Advances in management tools for modeling artificial nourishments in mixed beaches. J. Mar. Syst. 172, 1–13. https://doi.org/10.1016/j.jmarsys.2017.02.009.

Booij, N., Holthuijsen, L.H., Ris, R.C., 1996. The" SWAN" wave model for shallow water. Coast. Eng. Proc. 1, 668–676.

Bradbury, A.P., 2000. Predicting breaching of shingle barrier beaches: recent advances to aid beach management, in. In: Proceedings 35th MAFF (DEFRA) Conference of River and Coastal Engineers, pp. 1–15.

Bradbury, A.P., Orford, J.D., 2007. Influence of changing management regimes on the morphodynamic response, of a mixed gravel and sand barrier beach. In: Kraus, N.C., Rosati, J.D. (Eds.), Coastal Sediments 2007. ASCE, New Orleans, pp. 1–14. https://doi.org/10.1002/pros.22522.

Bradbury, A.P., Cope, S.N., Prouty, D.B., 2005. Predicting the response of shingle barrier beaches under extreme wave and water level conditions in Southern England. In: Fifth International Conference on Coastal Dynamics. https://doi.org/10.1061/40855(214)94.

Brooks, S.M., Spencer, T., McIvor, A., Möller, I., 2016. Reconstructing and understanding the impacts of storms and surges, southern North Sea. Earth Surf. Process. Landf. 41, 855–864. https://doi.org/10.1002/esp.3905.

Brooks, S., Spencer, T., Christie, E., 2017. Storm impacts and shoreline recovery: mechanisms and controls in the Southern North Sea. Geomorphology 283, 48–60. https://doi.org/10.1016/j.geomorph.2017.01.007.
Brown, S.I., Dickson, M.E., Kench, P.S., Bergillos, R.J., 2019. Modelling gravel barrier response to storms and sudden relative sea-level change using XBeach-G. Mar. Geol. 410, 164–175. https://doi.org/10.1016/j.margeo.2019.01.009.
Bujan, N., Cox, R., Masselink, G., 2019. From fine sand to boulders: examining the relationship between beach-face slope and sediment size. Mar. Geol. 417, 1–17. https://doi.org/10.1016/j.margeo.2019.106012.
Buscombe, D., Masselink, G., 2006. Concepts in gravel beach dynamics. Earth-Sci. Rev. 79, 33–52. https://doi.org/10.1016/j.earscirev.2006.06.003.
Carter, R.W.G., 1988. Coastal Environments – An Introduction to the Physical, Ecological and Cultural Systems of Coastlines. Academic Press, London, UK.
Carter, R.W.G., Orford, J.D., 1993. The morphodynamics of coarse clastic beaches and barriers: a short- and long-term perspective. J. Coast. Res. Special Is 158–179.
Carter, R.W.G., Orford, J.D., Forbes, D.L., Taylor, R.B., 1987. Gravel barriers, headlands, and lagoons: An evolutionary model. In: Kraus, N.C. (Ed.), Coastal Sediments 1987. American Society of Civil Engineers, New York, pp. 1776–1792.
Cattaneo, A., Steel, R.J., 2003. Transgressive deposits: a review of their variability. Earth-Sci. Rev. 62, 187–228.
Chaffin, B.C., Scown, M., Franke, W.A., 2018. Social-ecological resilience and geomorphic systems. Geomorphology 305, 221–230. https://doi.org/10.1016/j.geomorph.2017.09.038.
Channel Coastal Observatory, 2018. Regional Coastal Monitoring Programmes [WWW Document]. URL. http://www.channelcoast.org/ (accessed 12.1.18).
Church, M., 2010. The trajectory of geomorphology. Prog. Phys. Geogr. 34, 265–286. https://doi.org/10.1177/0309133310363992.
Clymo, R.S., 1967. Accretion rate in two of the salt marshes at Blakeney Point, Norfolk. Trans. Norfolk Norwich Nat. Soc. 21, 17–18.
Cooper, J.A.G., Green, A.N., Loureiro, C., 2018. Geological constraints on mesoscale coastal barrier behaviour. Glob. Planet. Chang. 168, 15–34. https://doi.org/10.1016/j.gloplacha.2018.06.006.
Cozens-Hardy, B., 1927. Cley-next-the-Sea and its marshes. Trans. Norfolk Norwich Nat. Soc. 12, 355–373.
Curray, J.R., 1964. Transgression and regression. In: Papers in Marine Geology. Macmillan Company, pp. 175–203.
Dale, J., Burgess, H.M., Cundy, A.B., 2017. Sedimentation rhythms and hydrodynamics in two engineered environments in an open coast managed realignment site. Mar. Geol. 383, 120–131. https://doi.org/10.1016/J.MARGEO.2016.12.001.
Davis, R.A., Andronaco, M., Gibeaut, J.C., 1989. Formation and development of a tidal inlet from a washover fan, west-central Florida coast, U.S.A. Sediment. Geol. 65, 87–94. https://doi.org/10.1016/0037-0738(89)90007-9.
de Vriend, H., Aarninkhof, S., van Koningsveld, M., 2014. 'Building with nature': the new Dutch approach to coastal and river works. In: Proceedings of the ICE - Civil Engineering, pp. 18–24. https://doi.org/10.1680/cien.13.00003.
DEFRA, 2018. DEFRA Data Services Platform [WWW Document]. URL. http://environment.data.gov.uk/ (accessed 12.1.18).
EACG (East Anglian Coastal Group), 2010. North Norfolk Shoreline Management Plan. Final Plan 2010. http://www.eacg.org.uk/docs/smp5/the%20smp%20main%20report.pdf.
Emery, A.R., Hodgson, D.M., Barlow, N.L.M., Carrivick, J.L., Cotterill, C.J., Mellett, C.L., Booth, A.D., 2019. Topographic and hydrodynamic controls on barrier retreat and preservation: an example from Dogger Bank, North Sea. Mar. Geol. 416.
Environment Agency, 2010. Shoreline Management Plan 5: Hunstanton to Kelling Hard.
Environment Agency, 2014. Sea State Report Norfolk Year 3 and Summary for October 2006 September 2009 (RP039/N/2014). Peterborough.
EurOtop, 2018. Manual on Wave Overtopping of Sea Defences and Related Structures An Overtopping Manual Largely Based on European Research, but for Worldwide Application Second Edition 2018.
Forbes, D.L., Syvitski, J.P.M., 1994. Paraglacial coasts. In: Carter, R.W.G., Woodroffe, C. D. (Eds.), Coastal Evolution: Late Quaternary Shoreline Morphodynamics. Cambridge University Press, Cambridge, pp. 373–424.
Forbes, D.L., Taylor, R.B., Orford, J.D., Carter, R.W.G., Shaw, J., 1991. Gravel-barrier migration and overstepping. Mar. Geol. 97, 305–313. https://doi.org/10.1016/0025-3227(91)90122-K.
Forbes, D.L., Orford, J.D., Carter, R.W.G., Shaw, J., Jennings, S.C., 1995. Morphodynamic evolution, self-organisation, and instability of coarse-clastic barriers on paraglacial coasts. Mar. Geol. 126, 63–85. https://doi.org/10.1016/0025-3227(95)00066-8.
Gohar, G., Bernie, D., Good, P., Lowe, J.A., 2018. UKCP18 Derived Projections of Future Climate over the UK [WWW Document].
Grabemann, I., Groll, N., Möller, J., Weisse, R., 2015. Climate change impact on North Sea wave conditions: a consistent analysis of ten projections. Ocean Dyn. 65, 255–267. https://doi.org/10.1007/s10236-014-0800-z.
Haff, P.K., 2003. Neogeomorphology, prediction, and the Anthropic landscape. In: Wilcock, P.R., Iverson, R.M. (Eds.), Prediction in Geomorphology, AGU Monograph Series, pp. 15–26. https://doi.org/10.1130/0091-7613(2000)28<843:OTHOHA>2.0.CO;2.
Haigh, I.D., Ozsoy, O., Wadey, M.P., Nicholls, R.J., Gallop, S.L., Wahl, T., Brown, J.M., 2017. An improved database of coastal flooding in the United Kingdom from 1915 to 2016. Sci. Data 4, 1–10. https://doi.org/10.1038/sdata.2017.100.
Hartstein, N.D., Dickinson, W.W., 2000. Gravel barrier migration and overstepping in Cable Bay, Nelson, New Zealand. J. Coast. Res. Special Is 256–266.
Hervouet, J.-M., 2000. TELEMAC modelling system: an overview. Hydrol. Process. 14, 2209–2210. https://doi.org/10.1002/1099-1085(200009)14:13<2209::AID-HYP23>3.0.CO;2-6.
Hinkel, J., Lincke, D., Vafeidis, A.T., Perrette, M., Nicholls, R.J., Tol, R.S.J., Marzeion, B., Fettweis, X., Ionescu, C., Levermann, A., 2014. Coastal flood damage and adaptation costs under 21st century sea-level rise. Proc. Natl. Acad. Sci. U. S. A. 111, 3292–3297. https://doi.org/10.1073/pnas.1222469111.
Hinkel, J., Aerts, J.C.J.H., Brown, S., Jiménez, J.A., Lincke, D., Nicholls, R.J., Scussolini, P., Sanchez-Arcilla, A., Vafeidis, A., Addo, K.A., 2018. The ability of societies to adapt to twenty-first-century sea-level rise. Nat. Clim. Chang. 8, 570–578. https://doi.org/10.1038/s41558-018-0176-z.
Holling, C., 1996. Engineering resilience versus ecological resilience. In: Engineering within Ecological Constraints. National Academy of Engineers, p. 214.
Hooke, R., 2000. On the history of humans as geomorphic agents. Geology 28, 843–846.
Hooton, J., 1996. The Glaven Ports: A Maritime History of Blakeney, Cley and Wiveton in North Norfolk. Blakeney History Group.
Horsburgh, K., Lowe, J., 2013. Impacts of climate change on sea level. Mar. Clim. Chang. Impacts Partnersh. Sci. Rev. 27–33 https://doi.org/10.14465/2013.arc04.027-033.
Hudson, C., Baily, B., 2018. Delivering sustainable coasts: monitoring the long-term stability of a breached barrier beach, Porlock Bay, Somerset, United Kingdom. Ocean Coast. Manag. 152, 88–99. https://doi.org/10.1016/j.ocecoaman.2017.11.022.
Inman, D.L., Brush, B.M., 1973. The coastal challenge. Science (80-.) 181, 20–32. https://doi.org/10.1126/science.181.4094.20.
Jäger, W.S., Christie, E.K., Hanea, A.M., Den Heijer, C., Spencer, T., 2018. A Bayesian network approach for coastal risk analysis and decision making. Coast. Eng. 134, 48–61. https://doi.org/10.1016/j.coastaleng.2017.05.004.
Jennings, R., Shulmeister, J., 2002. A field based classification scheme for gravel beaches. Mar. Geol. 186, 211–228. https://doi.org/10.1016/S0025-3227(02)00314-6.
Kabat, P., Fresco, L.O., Stive, M.J.F., Veerman, C.P., van Alphen, J.S.L.J., Parmet, B.W.A. H., Hazeleger, W., Katsman, C.A., 2009. Dutch coasts in transition. Nat. Geosci. 2, 450–452. https://doi.org/10.1038/ngeo572.
Kombiadou, K., Costas, S., Carrasco, A.R., Plomaritis, T.A., Ferreira, Ó., Matias, A., 2019. Bridging the gap between resilience and geomorphology of complex coastal systems. Earth-Sci. Rev. 198, 1–19. https://doi.org/10.1016/j.earscirev.2019.102934.
Lane, S.N., 2017. Slow science, the geographical expedition, and critical physical geography. Can. Geogr. / Le Géographe Can. 61, 84–101. https://doi.org/10.1111/cag.12329.
Lazarus, E.D., 2014. Threshold effects of hazard mitigation in coastal human–environmental systems. Earth Surf. Dynam 2, 35–45. https://doi.org/10.5194/esurf-2-35-2014.
Leatherman, S.P., 1979. Migration of Assateague Island, Maryland, by inlet and overwash processes. Geology 7, 104–107.
Leatherman, S.P., 1983. Barrier Island migration with Holocene sea level rise. Nature 301, 415–417.
Long, A.J., Waller, M.P., Plater, A.J., 2006. Coastal resilience and late Holocene tidal inlet history: the evolution of Dungeness Foreland and the Romney Marsh depositional complex (U.K.). Geomorphology 82, 309–330. https://doi.org/10.1016/j.geomorph.2006.05.010.
Lorenzo-Trueba, J., Ashton, A.D., 2014. Rollover, drowning, and discontinuous retreat: distinct modes of barrier response to sea-level rise arising from a simple morphodynamic model. J. Geophys. Res. Earth Surf. 119, 779–801. https://doi.org/10.1002/2013JF002941.
Masselink, G., Lazarus, E.D., 2019. Defining coastal resilience. Water 11, 1–21.
Masselink, G., Van Heteren, S., 2014. Response of wave-dominated and mixed-energy barriers to storms. Mar. Geol. 352, 321–347. https://doi.org/10.1016/j.margeo.2013.11.004.
Masselink, G., Ruju, A., Conley, D., Turner, I., Ruessink, G., Matias, A., Thompson, C., Castelle, B., Puleo, J., Citerone, V., Wolters, G., 2016. Large-scale barrier dynamics experiment II (BARDEX II): experimental design, instrumentation, test program, and data set. Coast. Eng. 113, 3–18. https://doi.org/10.1016/j.coastaleng.2015.07.009.
McCall, R.T., Masselink, G., Poate, T.G., Roelvink, J.A., Almeida, L.P., Davidson, M., Russell, P.E., 2014. Modelling storm hydrodynamics on gravel beaches with XBeach-G. Coast. Eng. 91, 231–250. https://doi.org/10.1016/j.coastaleng.2014.06.007.
McCall, R.T., Masselink, G., Poate, T.G., Roelvink, J.A., Almeida, L.P., 2015. Modelling the morphodynamics of gravel beaches during storms with XBeach-G. Coast. Eng. 103, 52–66. https://doi.org/10.1016/J.COASTALENG.2015.06.002.
McGranahan, G., Balk, D., Anderson, B., 2007. The rising tide: assessing the risks of climate change and human settlements in low elevation coastal zones. Environ. Urban. 19, 17–37. https://doi.org/10.1177/0956247807076960.
McNamara, D.E., Werner, B.T., 2008. Coupled barrier island-resort model: 1. Emergent instabilities induced by strong human-landscape interactions. J. Geophys. Res. Earth Surf. 113, 1–10. https://doi.org/10.1029/2007JF000840.
McRobie, A., Spencer, T., Gerritsen, H., 2005. The big flood: North Sea storm surge. Philos. Trans. A. Math. Phys. Eng. Sci. 363, 1263–1270. https://doi.org/10.1098/rsta.2005.1567.
Mellett, C.L., Hodgson, D.M.A.L., Mauz, B., Selby, I., Plater, A., 2012. Preservation of a drowned gravel barrier complex: a landscape evolution study from the north-eastern English Channel. Mar. Geol. 315–318, 115–131.
Mellett, C.L., Plater, A.J., 2018. Drowned barriers as archives of coastal-response to sea-level rise. In: Barrier Dynamics and Response to Changing Climate, pp. 57–90.
Miselis, J.L., Lorenzo-Trueba, J., 2017. Natural and human-induced variability in barrier-island response to sea level rise. Geophys. Res. Lett. 44, 11,922–11,931. https://doi.org/10.1002/2017GL074811.
Möller, I., 2019. Applying uncertain science to nature-based coastal protection: lessons from shallow wetland-dominated shores. Front. Environ. Sci. 7, 49. https://doi.org/10.3389/fenvs.2019.00049.

Moore, L.J., Murray, A.L., 2018. An overview of barrier dynamics. In: Moore, L.J., Murray, A.L. (Eds.), Barrier Dynamics and Response to Changing Climate. Springer, p. 420.
Muir Wood, R., Bateman, W., 2005. Uncertainties and constraints on breaching and their implications for flood loss estimation. Philos. Trans. A. Math. Phys. Eng. Sci. 363, 1423–1430. https://doi.org/10.1098/rsta.2005.1576.
Murray, A.B., Moore, L.J., 2018. Geometric constraints on long-term barrier migration: from simple to surprising. In: Moore, L.J., Murray, A.B. (Eds.), Barrier Dynamics and Response to Changing Climate. Springer, pp. 211–242.
Narayan, S., Hanson, S., Nicholls, R.J., Clarke, D., Willems, P., Ntegeka, V., Monbaliu, J., 2012. A holistic model for coastal flooding using system diagrams and the Source-Pathway-Receptor (SPR) concept. Nat. Hazards Earth Syst. Sci. 12, 1431–1439. https://doi.org/10.5194/nhess-12-1431-2012.
Naylor, L.A., Spencer, T., Lane, S.N., Darby, S.E., Magilligan, F.J., Macklin, M.G., Möller, I., 2017. Stormy geomorphology: geomorphic contributions in an age of climate extremes. Earth Surf. Process. Landf. 42, 166–190. https://doi.org/10.1002/esp.4062.
Neumann, B., Vafeidis, A.T., Zimmermann, J., Nicholls, R.J., 2015. Future coastal population growth and exposure to sea-level rise and coastal flooding - a global assessment. PLoS One 10, 1–34. https://doi.org/10.1371/journal.pone.0118571.
Nienhuis, J.H., Ashton, A.D., 2016. Mechanics and rates of tidal inlet migration: modeling and application to natural examples. J. Geophys. Res. Earth Surf. 121, 2118–2139. https://doi.org/10.1002/2016JF004035.
Nienhuis, J.H., Lorenzo-Trueba, J., 2019. Simulating barrier island response to sea-level rise with the barrier island and inlet environment (BRIE) model v1.0. Geosci. Model Dev. 12, 4013–4030. https://doi.org/10.5194/gmd-2019-10.
Nordstrom, K., 2000. Beaches and Dunes of Developed Coasts. Cambridge University Press, Cambridge, UK.
Odezulu, C.I., Lorenzo-Trueba, J., Wallace, D.J., Anderson, J.B., 2018. Follets Island: a case of unprecedented change and transition from rollover to subaqueous shoals. In: Moore, L.J., Murray, A.B. (Eds.), Barrier Dynamics and Response to Changing Climate. Springer, pp. 211–242.
Orford, J.D., 2011. Gravel-dominated coastal-barrier reorganisation variability as a function of coastal suseptibility and barrier resilience. In: The Proceedings of the Coastal Sediments, 2011, pp. 1257–1271.
Orford, J.D., Anthony, E.J., 2011. Extreme events and the morphodynamics of gravel-dominated coastal barriers: strengthening uncertain ground. Mar. Geol. 290, 41–45. https://doi.org/10.1016/j.margeo.2011.10.005.
Orford, J.D., Anthony, E., 2013. Coastal gravel systems. In: Treatise on Geomorphology. Academic Press, pp. 245–266.
Orford, J.D., Barry, L., 2016. Geomorphological advice in respect of Cley/Salthouse (North Norfolk) coastal gravel barrier changes, 2000-2014. In: Report 2B: Analysis on Mode and Extent of Barrier Changes. Belfast.
Orford, J.D., Carter, R.W.G., Jennings, S.C., 1991a. Gravel barrier migration and sea level rise: some observations from Story Head, Nova Scotia. Canada. J. Coast. Res. 7, 477–489.
Orford, J.D., Carter, R.W.G., Jennings, S.C., 1991b. Coarse clastic barrier environments: evolution and implications for quaternary sea level interpretation. Quat. Int. 9, 87–104. https://doi.org/10.1016/1040-6182(91)90068-Y.
Orford, J.D., Carter, R.W.G., Jennings, S.C., Hinton, A.C., 1995a. Processes and timescales by which a coastal gravel-dominated barrier responds geomorphologically to sea-level rise: Story head barrier, Nova Scotia. Earth Surf. Process. Landf. 20, 21–37. https://doi.org/10.1002/esp.3290200104.
Orford, J.D., Carter, R.W.G., McKenna, J., Jennings, S.C., 1995b. The relationship between the rate of mesoscale sea-level rise and the rate of retreat of swash-aligned gravel-dominated barriers. Mar. Geol. 124, 177–186. https://doi.org/10.1016/0025-3227(95)00039-2.
Orford, J., Carter, R.W., Jennings, S.C., 1996. Control domains and morphological phases in gravel-dominated coastal barriers of Nova Scotia. J. Coast. Res. 12, 589–604.
Orford, J., Forbes, D., Jennings, S., 2002. Organisational controls, typologies and time scales of paraglacial gravel-dominated coastal systems. Geomorphology 48, 51–85. https://doi.org/10.1016/S0169-555X(02)00175-7.
Orford, J.D., Jennings, S.C., Pethick, J.S., 2003. Extreme storm effect on gravel dominated barriers. In: Davis, R.A., Sallenger, A., Howd, P. (Eds.), Coastal Sediments 2003. World Scientific, Clearwater Beach, FL, pp. 1–14.
Orford, J., Barry, L., Collins, T., 2018. Can coastal gravel-dominated coastal barriers show persistent resilient morphological tuning to extreme storms? Geophys. Res. Abstr. 20, 2018–6041.
Palmer, M., Howard, T., Tinker, J., Lowe, J., Bricheno, L., Calvert, D., Edwards, T., Gregory, J., Harris, G., Krijnen, J., Pickering, M., Roberts, C., Wolf, J., 2018. UK Climate Projections 2018 Marine Report. Exeter.
Penland, S., Ramsey, K., 1988. Relative sea-level rise in Louisiana and the Gulf of Mexico: 1908-1988. J. Coast. Res. 6, 323–342. https://doi.org/10.2112/JCOASTRES-D-12-00.
Phillips, J.D., 1991. The human role in earth surface systems: some theoretical considerations. Geogr. Anal. 23, 316–331. https://doi.org/10.1016/B978-0-444-88826-6.50025-X.
Phillips, J.D., 2009. Changes, perturbations, and responses in geomorphic systems. Prog. Phys. Geogr. 33, 17–30.
Phillips, J.D., 2014. State transitions in geomorphic responses to environmental change. Geomorphology 204, 208–216. https://doi.org/10.1016/j.geomorph.2013.08.005.
Phillips, J., Van Dyke, C., 2016. Principles of geomorphic disturbance and recovery in response to storms. Earth Surf. Process. Landf. 41, 971–979. https://doi.org/10.1002/esp.3912.
Piégay, H., Chabot, A., Le Lay, Y.F., 2018. Some comments about resilience: from cyclicity to trajectory, a shift in living and nonliving system theory. Geomorphology. https://doi.org/10.1016/j.geomorph.2018.09.018.
Poate, T., Masselink, G., Davidson, M., McCall, R., Russell, P., Turner, I., 2013. High frequency in-situ field measurements of morphological response on a fine gravel beach during energetic wave conditions. Mar. Geol. 342, 1–13. https://doi.org/10.1016/j.margeo.2013.05.009.
Poate, T.G., McCall, R.T., Masselink, G., 2016. A new parameterisation for runup on gravel beaches. Coast. Eng. 117, 176–190. https://doi.org/10.1016/j.coastaleng.2016.08.003.
Pollard, M., 1978. North Sea Surge: The Story of the East Coast Floods of 1953. Terence Dalton Ltd, Lavenham, Suffolk.
Pollard, J.A., Christie, E.K., Brooks, S.M., Spencer, T., 2021. Impact of management regime and regime change on gravel barrier response to a major storm surge. J. Mar. Sci. Eng. 9, 1–25. https://doi.org/10.3390/jmse9020147.
Pollard, J.A., Spencer, T., Brooks, S.M., Christie, E.K., Möller, I., 2020. Understanding spatio-temporal barrier dynamics through the use of multiple shoreline proxies. Geomorphology 354 (107058). https://doi.org/10.1016/j.geomorph.2020.107058.
Rampino, M.R., Sanders, J.E., 1980. Holocene transgression in south-central Long Island (back barrier areas), New York. J. Sediment. Petrol. 50, 1063–1080. https://doi.org/10.1306/212F7B7B-2B24-11D7-8648000102C1865D.
Ranasinghe, R., Callaghan, D., Stive, M.J.F., 2012. Estimating coastal recession due to sea level rise: beyond the Bruun rule. Clim. Chang. 110, 561–574. https://doi.org/10.1007/s10584-011-0107-8.
Ranjan, P., Kazama, S., Sawamoto, M., Sana, A., 2009. Global scale evaluation of coastal fresh groundwater resources. Ocean Coast. Manag. 52, 197–206.
Rodriguez, A.B., Yu, W., Theuerkauf, E.J., 2018. Abrupt increase in washover deposition along a transgressive barrier island during the late nineteenth century acceleration in sea-level rise. In: Moore, L.J., Murray, A.B. (Eds.), Barrier Dynamics and Response to Changing Climate. Springer, pp. 121–145.
Rogers, L.J., Moore, L.J., Goldstein, E.B., Hein, C.J., Lorenzo-Trueba, J., Ashton, A.D., 2015. Anthropogenic controls on overwash deposition: evidence and consequences. J. Geophys. Res. F Earth Surf. 120, 2609–2624. https://doi.org/10.1002/2015JF003634.
Sallenger, A.H., 2000. Storm impact scale for Barrier Islands. J. Coast. Res. 16, 890–895. https://doi.org/10.2307/4300099.
Sayers, P.B., Hall, J.W., Meadowcroft, I.C., 2002. Towards risk-based flood hazard management in the UK. Proc. Inst. Civ. Eng. - Civ. Eng. 150, 36–42. https://doi.org/10.1680/cien.2002.150.5.36.
Schuerch, M., Spencer, T., Temmerman, S., Kirwan, M.L., Wolff, C., Lincke, D., McOwen, C.J., Pickering, M.D., Reef, R., Vafeidis, A.T., Hinkel, J., Nicholls, R.J., Brown, S., 2018. Future response of global coastal wetlands to sea-level rise. Nature 561, 231–234. https://doi.org/10.1038/s41586-018-0476-5.
Spalding, M.D., McIvor, A.L., Beck, M.W., Koch, E.W., Möller, I., Reed, D.J., Rubinoff, P., Spencer, T., Tolhurst, T.J., Wamsley, T.V., van Wesenbeeck, B.K., Wolanski, E., Woodroffe, C.D., 2014. Coastal ecosystems: a critical element of risk reduction. Conserv. Lett. 7, 293–301. https://doi.org/10.1111/conl.12074.
Spencer, T., Brooks, S.M., Evans, B.R., Tempest, J.A., Möller, I., 2015. Southern North Sea storm surge event of 5 December 2013: water levels, waves and coastal impacts. Earth-Sci. Rev. 146, 120–145. https://doi.org/10.1016/j.earscirev.2015.04.002.
Spencer, T., Brooks, S.M., Pollard, J.A., 2020. The Barrier Coastline of North Norfolk, with particular reference to Scolt Head Island. In: Goudie, A., Migoń, P. (Eds.), Landscapes and Landforms of England & Wales. Springer, pp. 359–380.
Stallins, J.A., 2005. Stability domains in barrier island dune systems. Ecol. Complex. 2, 410–430. https://doi.org/10.1016/j.ecocom.2005.04.011.
Stéphan, P., Suanez, S., Fichaut, B., Stéphan, P., Brest-iroise, T., Copernic, P.N., 2012. Long-term morphodynamic evolution of the Sillon de Talbert gravel barrier (Brittany, France). Shore Beach 80, 19–36.
Stéphan, P., Suanez, S., Fichaut, B., Autret, R., Blaise, E., Houron, J., Ammann, J., Grandjean, P., 2018. Monitoring the medium-term retreat of a gravel spit barrier and. Ocean Coast. Manag. 158, 64–82. https://doi.org/10.1016/j.ocecoaman.2018.03.030.
Stolper, D., List, J.H., Thieler, E.R., 2005. Simulating the evolution of coastal morphology and stratigraphy with a new morphological-behaviour model (GEOMBEST). Mar. Geol. 218, 17–36. https://doi.org/10.1016/j.margeo.2005.02.019.
Stripling, S., Bradbury, A.P., Cope, S.N., Brampton, A.H., 2008. Understanding barrier beaches. In: R&D Technical Report FD1924/TR. DEFRA, London, pp. 1–318.
Stutz, M.L., Pilkey, O.H., 2011. Open-ocean barrier islands: global influence of climatic, oceanographic, and depositional settings. J. Coast. Res. 27, 207–222. https://doi.org/10.2112/09-1190.1.
Sutherland, J., Peet, A.H., Soulsby, R.L., 2004. Evaluating the performance of morphological models. Coast. Eng. 51, 917–939. https://doi.org/10.1016/j.coastaleng.2004.07.015.
Swift, D.J.P., Moslow, T., 1982. Holocene transgression in south-central Long Island, New York — discussion. J. Sediment. Petrol. 52, 1014–1019.
Swift, D.J.P., Phillips, S., Thorne, J., 1991. Sedimentation on continental margins, V: parasequences. In: Swift, D.J.P., Oertel, G.F., Tillman, R.W., Thorne, J.A. (Eds.), Shelf Sand and Sandstone Bodies— Geometry. Facies and Sequence Stratigraphy. International Association of Sedimentology Special Publication, pp. 153–187.
Thoms, M.C., Piégay, H., Parsons, M., 2018. What do you mean, "resilient geomorphic systems"? Geomorphology 305, 8–19. https://doi.org/10.1016/j.geomorph.2017.09.003.
UK Hydrographic Office, 2018. Offshore bathymetry products [WWW Document]. URL. https://www.gov.uk/guidance/inspire-portal-and-medin-bathymetry-data-archive-centre#about-the-admiralty-marine-data-portal (accessed 12.1.18).

Vitousek, S., Barnard, P.L., Fletcher, C.H., Frazer, N., Erikson, L., Storlazzi, C.D., 2017. Doubling of coastal flooding frequency within decades due to sea-level rise. Sci. Rep. 7, 1399. https://doi.org/10.1038/s41598-017-01362-7.

Vousdoukas, M.I., Voukouvalas, E., Annunziato, A., Giardino, A., Feyen, L., 2016. Projections of extreme storm surge levels along Europe. Clim. Dyn. 47, 3171–3190. https://doi.org/10.1007/s00382-016-3019-5.

Vousdoukas, M.I., Mentaschi, L., Feyen, L., Voukouvalas, E., 2017. Extreme sea levels on the rise along Europe's coasts. Earth's Futur. 5, 304–323. https://doi.org/10.1002/eft2.192.

Wahl, T., Haigh, I.D., Woodworth, P.L., Albrecht, F., Dillingh, D., Jensen, J., Nicholls, R. J., Weisse, R., Wöppelmann, G., 2013. Observed mean sea level changes around the North Sea coastline from 1800 to present. Earth-Sci. Rev. 124, 51–67. https://doi.org/10.1016/J.EARSCIREV.2013.05.003.

Werner, B.T., McNamara, D.E., 2007. Dynamics of coupled human-landscape systems. Geomorphology 91, 393–407. https://doi.org/10.1016/j.geomorph.2007.04.020.

White, D.B., 1979. The effects of the storm of 11th January 1978 on Blakeney Point. Trans. Norfolk Norwich Nat. Soc. 25, 267–269.

Williams, J.J., Buscombe, D., Masselink, G., Turner, I.L., Swinkels, C., 2012. Barrier dynamics experiment (BARDEX): aims, design and procedures. Coast. Eng. 63, 3–12. https://doi.org/10.1016/j.coastaleng.2011.12.009.

Woth, K., Weisse, R., Von Storch, H., 2006. Climate change and North Sea storm surge extremes: an ensemble study of storm surge extremes expected in a changed climate projected by four different regional climate models. Ocean Dyn. 56, 3–15. https://doi.org/10.1007/s10236-005-0024-3.

Wright, L.D., Short, A.D., 1984. Morphodynamic variability of surf zones and beaches: a synthesis. Mar. Geol. 56, 93–118. https://doi.org/10.1016/0025-3227(84)90008-2.